Environmental Science and Pollution Research (2021) 28:43287–43314
https://doi.org/10.1007/s11356-021-14707-7

REVIEW ARTICLE

Fractal approach in expansive clay-based materials with special focus on compacted GMZ bentonite in nuclear waste disposal: a systematic review

Fazal E. Jalal[1] · Yongfu Xu[1,2] · Xiaoyue Li[1] · Babak Jamhiri[1] · Mudassir Iqbal[1]

Received: 5 April 2021 / Accepted: 31 May 2021 / Published online: 29 June 2021

Abstract

Knowledge of the behavior of highly compacted expansive clays, as an engineered barrier, in disposal of high-level nuclear waste (HLW) systems to prevent the pollution due to migration of radionuclide is extremely essential. The prominent properties of globally and widely used bentonites have been extensively studied during past two decades. In China, GaoMiaoZi (GMZ) bentonite is the first choice as a buffer or backfill material for deep geological repositories. This review article presents the recent progresses of knowledge on water retention properties, hydromechanical behavior, and fractal characteristics of GMZ bentonite-based materials, by reviewing 217 internationally published research articles. Firstly, the current literature regarding hydrogeochemical and mechanical characteristics of GMZ bentonite influenced by various saline solutions are critically summarized and reviewed. Then, the role of osmotic suction π alongside the application of surface fractal dimension D_s is presented from the standpoint of fractal theory. Finally, the strength characteristics of GMZ bentonites using fractal approach have been discussed. Furthermore, this study sheds light on gaps, opportunities, and further research for understanding and analyzing the long-term hydromechanical characteristics of the designed backfill material, from the standpoint of surface fractality of bentonites, and implications of sustainable buffer materials in the field of geoenvironmental engineering.

Keywords Expansive clays, · GMZ bentonite, · Hydromechanical behavior, · Osmotic suction, · Surface fractal dimension (D_s), · Fractal theory

Introduction

Expansive clays such as bentonites have numerous applications in the construction industry and deep nuclear waste disposal systems to deal with municipal solid wastes (MSWs) (Gens 2019; Ray et al. 2021). Bentonites are mainly Na-bentonites and Ca-bentonites. Sodic type has more swelling capacity than calcic bentonites because of lesser hydration energy of exchangeable monovalent (Na^+) cations (Cui 2017). Other general applications of bentonites include drilling fluids, cosmetic formulations, and use as natural multivitamin (Churchman et al. 2002). Montmorillonite (from hereon referred to as Mt) clay mineral, having less than 2-μ particle size, is the main ingredient of natural bentonite with traces of cristobalite, crystalline quartz, and feldspar (Barakan and Aghazadeh 2020). It has an overall negative charge due to the isomorphous substitution and is responsible for the water uptake and swelling phenomena. It has alternating layered structure of silicon oxygen tetrahedron and hydroxyl octahedral (T-O-T) with six OH and four O_2 molecules (Fattah and Al-Lami 2016; Jalal et al. 2020; Jiang et al. 2014; Rao et al. 2013; Uddin 2008; Ye et al. 2014) as shown in Fig. 1a. Bentonite is famous for providing waterproofing capabilities in leachate liners and in contributing to swelling impedance in bentonite-based materials (BBMs) (Pathak 2017; Reijonen et al. 2020). The swelling mechanism of BBMs resembles that of pure bentonites (Liu 2013). Highly expansive clays tend to produce negative electric charge in water that is capable of adsorbing any positively charged toxins (Miazzo et al.

Responsible Editor: Philippe Garrigues

✉ Yongfu Xu
yongfuxu@sjtu.edu.cn

[1] Department of Civil Engineering, State Key Laboratory of Ocean Engineering, Shanghai Jiao Tong University, Shanghai 200240, China

[2] Wanjiang Institute of Technology, Ma'anshan 243000, China

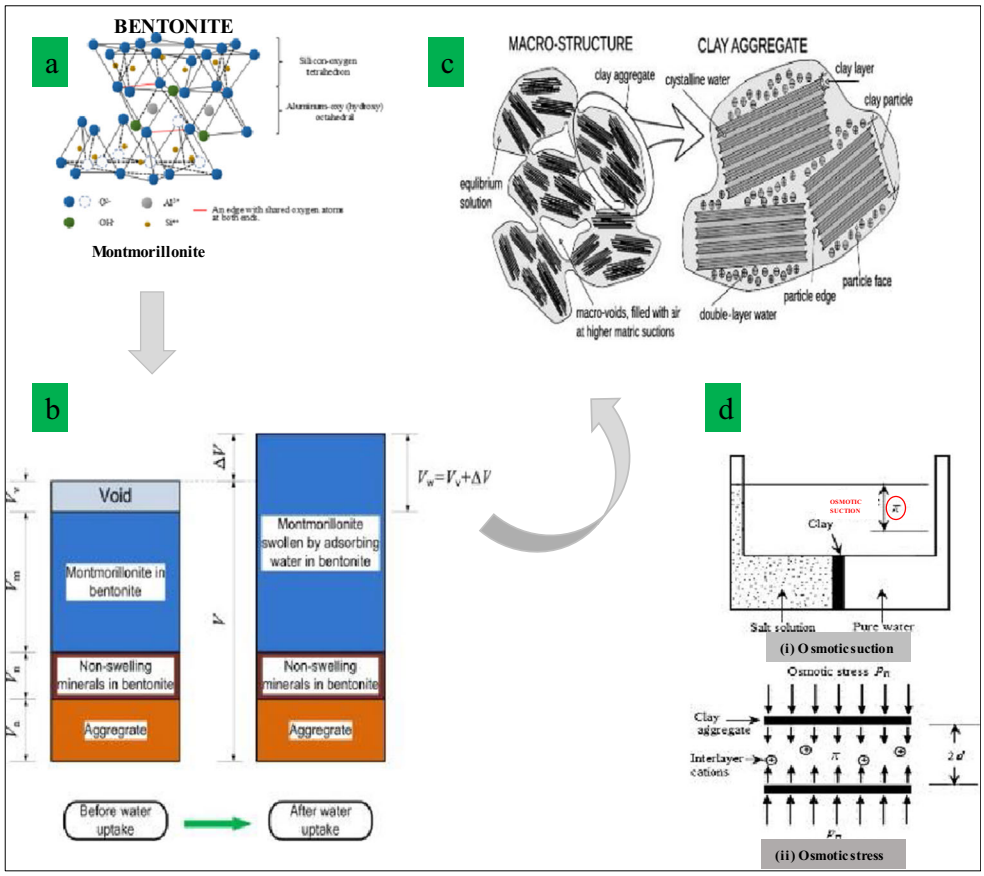

Fig. 1 Water uptake process in bentonite is shown schematically alongside the microstructural changes in swelling phenomenon, adapted from (Liu 2013; Mašín and Khalili 2015; Xu 2019) with modification

2005), as visulized in Fig. 1a to c. In addition, BBMs exhibit low hydraulic conductivity, high swelling potential, better self-sealing ability, good gas release capacity and rheological properties and enhanced radionuclide retardation capacity (He et al. 2019a; Liu et al. 2020; Liu 2013; Pusch 1999; Wang 2010). Expansive soils are function to total suction (h_t or Ψ) comprises two major components i.e., matric (h_m) and osmotic suctions (h_π or π) and can be measured by experiments or analytical techniques (Mokni et al. 2014). Also, the swelling pressure (P_s) of bentonites is governed by both the components of total suction. The swelling pressure induced by the hydration of cations and surfaces of the clay platelets is called crystalline swelling (Xu 2018). Subsequent swelling induced after completion of crystalline swelling is attributed to the osmotic process and is called the osmotic or double layer swelling (Liu 2013) (Fig. 1d). Osmotic suction component comes from dissolved solutes in soil pore-water and bentonites. It is also shown in Fig. 1d that the clay particles of bentonite also exhibit an inherent osmotic suction because of ions present in their pore water. Osmotic pressure can be determined by employing the thermodynamic principles and the Van't Hoff equation (Leong and Abuel-Naga 2018; Li and Xu 2020; Rao and Shivananda 2005; Xu et al. 2014).

Furthermore, in geoenvironmental engineering, bentonites are used for lining of dams and for the disposal of high level nuclear waste (HLW) disposal in the form of buffer material across the globe (Arifin et al. 2015; Cui 2017; Dixon 2000; Kaufhold et al. 2015; Kim et al. 2019; Komine 2004a; Komine 2004b; Pusch 1999; 2015; Siddiqua et al. 2011; Stewart et al. 2003; Sun et al. 2017; Tripathy et al. 2015; Villar and Lloret 2004; Wieczorek et al. 2017; Xu 2003; Xu et al. 2003). Fig. 2a and b illustrates the mechanism of underground geological repository for disposal of HLW within a bentonite clay buffer. Highly expansive clays such as bentonites play a key role in the various stages of the deep geological disposal of high-level nuclear waste (Christopher and Chimobi 2019; Gens 2019). Different materials are used in engineered barrier system (EBS), such as vitrified nuclear waste, canister, buffer as well as backfill materials in the construction of artificial barrier to form deep geological repository (DGR) (Zhi-jian 2009). Fig. 2c illustrates the canisters, backfill, near-field rock and buffers in the EBS. The buffers are filling materials, for instance bentonite-based materials, between the canister and the disposal hole. The buffers used here are designed to protect the canisters from shearing effects of nearby rocks, to suppress microbial activity, and to inhibit the leakage of nuclides by reducing groundwater inflow (Baltrėnaitė et al. 2018; Briggs et al. 2017; Yoon et al. 2019).

According to 3-stages Chinese HLW disposal program initiated in the late 1980s, the major objectives were (i) to select

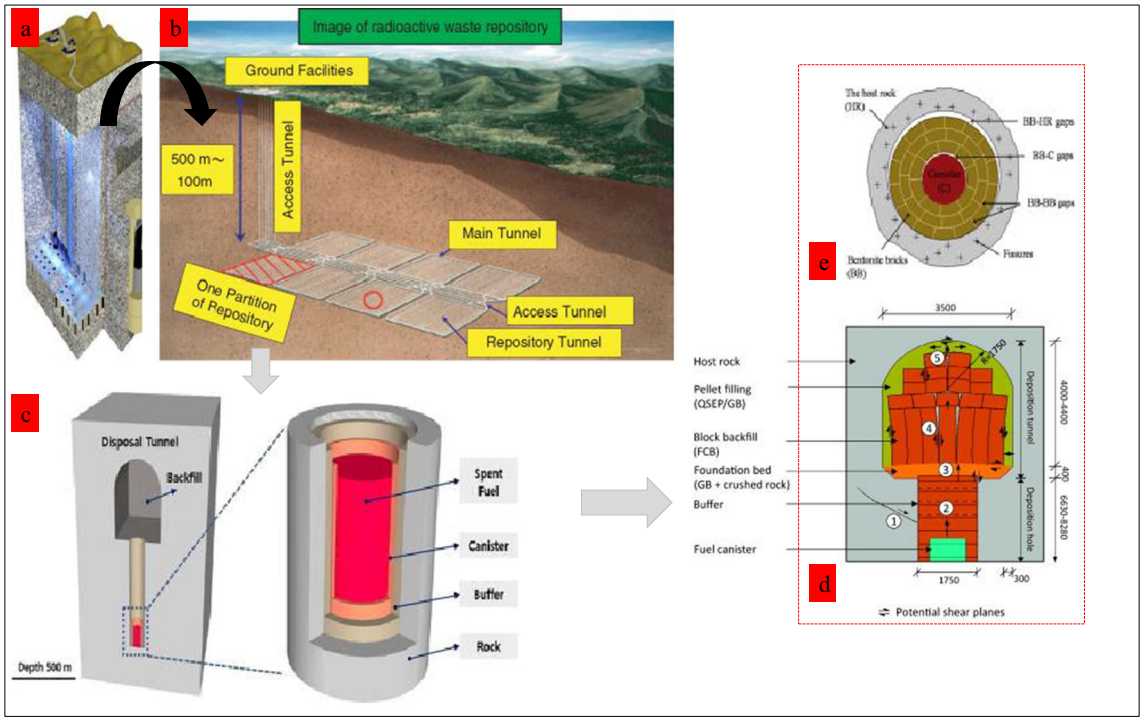

Fig. 2 Schematic of underground geological repository for high-level radioactive waste disposal with gaps/cracks developed in bentonite bricks overtime, modified after (Jia et al. 2019; Sinnathamby et al. 2015; Yokozeki 2007; Yoon et al. 2019)

site and construct underground research laboratory (2006–2020), (ii) to conduct underground in-situ tests (2021–2040), and (iii) to complete the first geological repository using vitrified HLW (2041–2050). In the HLW disposal system, the hazardous and nuclear waste accumulates in the interim storage facilities and therefore the final waste repositories are established for efficacious disposal of radioactive waste in the form of waste-filled-canisters at greater depths (500~1000 m below the ground surface) (Wang 2010; Xu 2018; Zhang et al. 2016).

The mechanical behavior of clay is largely affected by the pore fluid composition since the clay particles are electrically charged (Li et al. 2019, n.d.; Xu et al. 2014). Ye et al. (2010b) studied the influence of salinity and salinization-desalinization phenomena on the swelling properties of heavily compacted GMZ01 bentonite by incorporating NaCl, $CaCl_2$ and KCl (0.5 and 2 M). Furthermore, it was found by Yu et al. (2019) that soil compressibility, strength, and hydraulic conductivity of the buffer material are largely affected by the soil suction. For known total suction of ~~the~~ clay, the specimen inundated in high concentration solution exhibits a larger h_π and thus has a smaller value of h_m (He et al. 2016; Nowamooz and Masrouri 2010). The increasing h_π of the solution concentration tends to weaken the clay swelling in containment of HLW repository. Moreover, the higher h_π at elevated temperature and high solution concentration may enlarge the decrease in the P_s (Chen et al. 2018). The h_π due to high saline solutions may also slightly reduce the P_s of bentonite-based buffer materials (Castellanos et al. 2008). The sodic montmorillonite is more sensitive to osmotic phenomenon in contrast to the K-montmorillonite and Ca-montmorillonite owing to their smaller double layers. In addition, the blending of NaCl, $CaCl_2$, KCl in the bentonites produced ion diffusion into the pore fluid resulting in reduced volume which increased the residual shear strength mainly due to osmotic consolidation (Di Maio 1996). Zhang et al. (2016) found that, the shear strength undergoes a noticeable improvement with increasing NaCl concentration (0, 0.2, 0.5, 1 and 2 mol/L) and concluded that the internal friction angle increases fairly, whereas cohesion remains almost unchanged. Li et al. (2019) proved a uniform relationship of the volume change and the modified effective stress equation in various saline solutions (NaCl, $CaCl_2$, $NaNO_3$, Ca $(NO_3)_2$) using a unique equation that validates the modified effective stress concept.

The concept of fractals quantifies the complexity of surface topographies and disordered objects on the basis of self-similarity among the surfaces at various scales. Benoit Mandelbrot introduced the term "fractal," meaning "to fragment" and "irregular" implying to broken or fractured for the self-similar geometric figures which scale a dimension in whole number powers, e.g., Sierpinski triangle is 1.262 dimensional and Von Koch snowflake is 1.585 dimensional, whereas, the value for soil particles is between 2 and 3 (Lathrop et al. 2009; Mandelbrot 2013; Mandelbrot 1983; Young et al. 2001). Fractal is that object whose dimensionality lies midway (i.e., 1 and 2, 2 and 3, etc.), such as, 1.3

dimension refers to an uneven line, whereas, an object having 2.2 dimension represents a surface (He 2016). In case of smooth boundary, the fractal dimension of the object will be close to unity, while for a rougher boundary the fractal dimension approaches equal to two (Castillo and Melin 2020). Fractal dimension in variety of clays has been used to represent the water retention, grain size distribution, and the mechanical performance under impact loading of the soils (Yang and Wang 2020). The surface fractal dimension (from hereon referred to as SFD or D_s) of expansive clay serves to characterize the surface roughness or irregularities of clay particles surfaces. Furthermore, the surface irregularity and roughness of bentonite also directly affect its heavy metal adsorption performance. The magnitude of the SFD is relevant to many vital physico-chemical processes, for example, adsorption, surface diffusion and catalysis. The lower value indicates a smooth surface while the higher value suggests that the surface is rough (Peng et al. 2020; Xu et al. 2014). The D_s helps to characterize the microstructure of porous materials such as soils, rocks, ceramic gels and cement pastes (Zeng et al. 2013). The microstructure of expansive clays can be quantified by fractals because the DDL theory assumes smooth surface of Mt regardless of the rough surface of bentonite thus relating the swelling characteristics with fractals (Xiang et al. 2014b; Xu and Liu 1999). Modified effective stress incorporates the effect of osmotic suction and has been found to follow fractal nature by exhibiting a unique straight line on logarithmic plot. The volume change behavior of bentonite or expansive soils is represented by the unique curve using the proposed effective stress for the bentonites in saline solution having various concentration levels. The proposed subsequent formula is based on fractal model for the surface of clay structure such that osmotic suction is determined from the Van't Hoff equation and the volume change behavior of expansive soils can be expressed by the aforementioned curve of $e–p^e$ which is also validated by experimental data (Xu et al. 2014; Zhang et al. 2013). From the standpoint of salinity of solutions, the D_s is highly related to the h_π of the compacted mixture, for instance, in the calculation of peak shear strength of saline solutions (Xiang et al. 2019b). The effect of h_π has been explained quantitatively after determining the D_s of Tsukinuno bentonite by nitrogen adsorption test and a modified form of the effective stress has been proposed which incorporates the effect of the h_π (Xu et al. 2014).

Numerous research are available on application of fractal theory in determining soil properties in general; along with some special focus on the effect of D_s on the hydro-mechanical nature of expansive soils (Li and Xu 2020; Li et al. 2019; Liu et al. 2014; Mandelbrot 1983; Schanz and Al-Badran 2014; Xiang et al. 2015; 2019b; Xu 2019; Xu et al. 2003; Xu et al. 2004; Ye et al. 2009).Therefore, on the basis of established applications of GMZ as bentonite buffer material in geological repositories with respect to swelling behavior, hydraulicity properties and mechanical characteristics, a review on fractal theory approaches is presented. This review article takes into consideration the progresses made on hydrochemomechanical behavior and the efficacy of fractal theory for the GMZ based materials, which has not been addressed till date. The main objectives to determine these properties include (a) hydrogeochemical and mechanical characteristics influenced by various saline solutions to assess buffering materials, and (b) the role of osmotic suction and application of surface fractal dimension D_s., and (c) the effects on the volume change and compression characteristics based on previous studies pertaining to GMZ bentonite. In addition, the standby problems needing solutions and the key points and frequent issues that should be addressed in future are also suggested for GMZ bentonite-based materials.

Basic properties of prominent bentonites in the world

Some of the physical, chemical and mineralogical properties of global bentonites, including GMZ, are presented in Table 1. It is evident that sodic bentonites exhibit an overall better performance than the calcic bentonites in terms of usage as potential buffer material in the deep geological repositories. It can be observed that the liquid limit (LL) and plasticity index (PI) of Na-bentonites are almost three times and five times that of Ca-bentonites, respectively. The LL and PI tests are conducted according to ASTM D-4318 standard for determining the water-holding capacity of clays. Also, the values of LL and PI for volclay bentonites are the highest of all and reported as 628% and 583%, respectively. Note that, according to Horpibulsuk et al. (2011) the reduction of the LL is generally caused by the compression of DDL. Furthermore, the SFD for Na-bentonite has lower values (D_s = 2.55 to 2.67) than those of Ca-bentonite (D_s = 2.67 to 2.80), while the D_s values of Ponza and FoCa7 bentonites are reported to be 2.55 and 2.80, respectively. The decrease in D_s is an indicator of the complex behavior of pore system Liu et al. (2014). The Mt amount in GMZ is comparatively lesser than that in Febex and MX-80, whereas, it is higher than that of Kunigel VI, which according to Liu (2010), leads to establishing reliable correlations between the Mt content and cation exchange capacity (CEC) of respective bentonites. Ye et al. (2014) argued that, Mt content is directly related to CEC value of bentonites. Xiang et al. (2019b) studied that, the diffusion of alkaline solutes into bentonite-based mixtures dissolves Mt mineral which will weaken the properties of the bentonite, as pH is raised to 13–14 (Liu et al. 2018). However, according to another study by Herbert et al. (2008), after reaction with alkaline solution the Mt aggregates were broken apart between MX-80 bentonite and alkaline solution after elapsed time of 3 years. The

Table 1 Physical and chemical properties of globally predominant bentonites in practice

Country	Bentonite	Deposit	Content of:		Dominant content of:		Particle density	LL	PL	PI	Amount of exchange cations:				CEC	SSA	D_s
			Smectite	Clay	Smectite	Exch. Cation					Na	Ca	K	Mg			
			%	%			Mg/m^3	%	%	%	meq/100mg					m^2/g	
Japan	Kunibond	Dobuyama Mine	80	64.5	Mt	Ca	2.71	145	64	81	7	12	59	2	80	-	-
(Komine 2004a; Mašín and Khalili 2015; Xu 2018; Zhi-jian 2005)	Kunigel VI	Tsukinuno Mine	48	71.5	Mt	Na	2.79	474	27	447	3	41	29	0	73	687	2.62
	Neokunibond	Kawasaki-cho Mine	76	78	Mt	Artificial Na	2.68	607	51	556	6	62	33	3	104	-	-
USA	MX-80	Wyoming	83	91.9	Mt	Na	2.76	519	35	484	5	67	8	8	88	522	2.62
(Komine 2004a; Mašín and Khalili 2015; Xu 2018)	Volclay	Wyoming	69	-	Mt	Na	2.84	628	45	583	13	57	29	2	101	-	-
Germany	Montigel	Bavaria	62	40	Mt	Ca	2.85	130	50	80	9	33	0	32	[b]74	493	2.73
(Arifin et al. 2015; Xu 2018)	Calcigel	-	55	80	Mt	Ca	2.65	130	33	97	-	-	-	-	49	69	2.72
Italy (Calvello et al. 2005; Di Maio et al. 2004; DI MAIOĆ 1996; Xu 2018)	Ponza	Ponza and Gavi	75		Mt	Na	2.77	390	70	320	-	-	-	-	40	500	2.55
	Bisaccia	Bisaccia	30	60	Mt+K+I	Ca	2.78	110	-	-	-	-	-	-	42	190	2.67
China (Arifin et al. 2015; Sun et al. 2018; Xu 2018; Ye et al. 2014)	GMZ01	Inner Mangolia	76	60	Mt	Ca	2.66	276	37	239	12	35	23	1	71	[c]597	2.78
	GMZ07	Inner Mangolia	63	68	Mt	Ca	2.76	125	30	95	-	-	-	-	42	570	2.78
Spain (Arifin et al. 2015; Cui et al. 2011; Villar and Lloret 2004; Villar and Lloret 2008; Xu 2018)	Serrata clay or FEBEX	Cortijo de Archidona	92	68	Mt	Ca	2.70	a102	a53	49	31	27	42	2	102	725	2.8
France, Belgium (Arifin et al. 2015; Mašín and Khalili 2015; Xu 2018)	FoCa7	Fourges Cahaignes	80	-	B+K	Ca	2.67	112	50	62	2	3	63	1	69	300	2.8
Canada (Mašín and Khalili 2015; Xu 2018)	Avonseal	Saskatchewan	79	83	Mt	Na	-	240	40	200	6	41	35	0	82	550	2.67
India (Arifin et al. 2015)	Indian	-	-	70	-	Ca	2.85	400	34	366	-	-	-	-	62	400	-
Indonesia (Arifin et al. 2015)	Indonesian	Commercial	-		Mt+I	Ca	2.78	140	55	85	-	-	-	-	27	-	-

Note: B, Beidelite; K, Kaolinite; I, Illite

The montmorillonite (Mt) content was determined using methylene blue absorption values of the respective bentonite and Mt.

[a] (Cui et al. 2008) ; [b] (Liu 2013) ; [c] (Zhi-jian 2005)

temperature also has a significant impact on bentonite corrosion in saline solution (Xiang et al. 2019b).

The artificial neural network (ANN) analysis was performed on the data given in Table 1, by considering smectite (%), particle density (Mg/m^3), PI (%), CEC (meq/100mg) and SSA (m^2/g) as input, while D_s as the output variable. The details of performing ANN analysis are outlined elsewhere (Das 2013; Sathyapriya et al. 2017; Shahin 2013). The model was trained using Levenberg-Marquardt method and the number of hidden neurons were selected as 10. The dataset was divided into 60% training, 20% validation and 20% testing data for the formulation of ANN model, in accordance with the requirement of a minimum ratio of 3 (and, preferably > 5) between data points and input variables, as stated by Gandomi and Roke (2015). A strong overall correlation coefficient (*R*) of 81% (Iqbal et al. 2020) was recorded between the observed and predicted values (Fig. 3). The *R* values measure the correlation between outputs and targets and an R value of 1 means a strong relationship, while zero represents no relationship. The mean absolue error (MAE) was 0.042. MAE is the average squared difference between outputs and targets. Lower values are better whereas zero means no error. Various evaluation criteria, i.e., Nash-Sutcliffe efficiency (NSE) (Shah et al. 2020), root mean square error (RMSE) (Jalal et al. 2021), and performance index (P_i) (Iqbal et al. 2020) were used to assess the performance of the ANN model (Raheem et al. 2017; Shah et al. 2020). The values of aforementioned indices were determined using proposed equations in literature and are also tabulated in the Fig. 3. All values can be seen to lie in permissible limits required for an optimum neural model (Shahin et al. 2009).

The elemental composition of 25 global bentonites determined by the X-ray fluorescence (XRF) test is listed in Table 2. It is observed that, the average range of silica, iron oxide and alumina is between 50 – 60%, 1 – 10%, and 12–30%, respectively. Quartz or SiO_2 is an imperative mineral that significantly affects the thermal conductivity of highly expansive clays (Cui et al. 2011; Tang et al. 2008). According to the definition of a pozzolan by the ASTM, all the listed bentonites are "pozzolanic" in nature since the cumulative percentage of SiO_2+Al_2O_3+Fe_2O_3 exceeds 70% (Agarwal 2006; Mohammed 2017).

GaoMiaoZi bentonite

The GaoMiaoZi bentonite has proved to be a reliable material for Chinese geological repository located in Beishan area of Gansu province (Fig. 4) (Zuo et al. 2019). The GMZ bentonite (GMZ01, GMZ07) has been the first choice for use as buffer or backfill material owing to its hydrophilic character and good sealant characteristics (He et al. 2019b; Schanz and Al-Badran 2014; Xu 2019; Ye et al. 2013; Zhang et al. 2019a). For determining the suction of GMZ bentonite-sand mixtures, pressure plate method and the filter paper method were previously used (Meng et al. 2012). Note that, the GMZ bentonites are mainly classified as GMZ01 and GMZ07 which are extracted from different sources in Wulanchabu city of northern Chinese Inner Mongolia autonomous region, 800 km from Beijing (He et al. 2019b; Sun et al. 2020; Ye et al. 2013; Zhang et al. 2019b). According to the small-angle X-ray scattering (SAXS) technique, scattering intensity of GMZ01 is smaller than that of GMZ07 while both have similar fractal dimensions with pore size reported to be much concentrated and a higher P_s is recorded in the former type (Long et al. 2016). The SAXS technique is based on the difference in electron density and is capable to detect the interlayer pores of the Mt (Peng et al. 2020). The difference in the mechanical behavior of the two types is attributed to the grain size and the amount of Mt content (Long et al. 2016). The expansivity properties of the sodic and calcic GMZ bentonites are approximately equal in the range of higher densities (Sun and Fang 2014). The physical properties of the GMZ bentonite and the ground water characteristics in the geological repository site of Beishan (with granite as host rock) are also shown in Fig. 4 (Liu et al. 2001; Sun et al. 2018; Wang 2010; Ye et al. 2014).

GMZ bentonite exhibits large thermal conductivity (1.51 W/mK at ρ_d =1.6 Mg/m^3 , ω = 27%), greater SSA (570 m^2/g), reduced saturated hydraulic conductivity (k_{sat} = 1.94 x 10^{-13} m/s at ρ_d =1.6 Mg/m^3 and 25 °C), large CEC (77.30 meq/100 g), higher (11.7%) quartz content, high liquid limit LL= 313% and plastic limit PL=38%, greater UCS (1740 kPa at ρ_d =1.6 Mg/m^3 , ω = 24%), relatively large P_s (3170 kPa at ρ_d =1.6 Mg/m^3), and specific gravity G_s = 2.66 (Cui et al. 2011; Ye et al. 2014).

The X-ray diffraction (XRD) analysis is commonly conducted to investigate the mineralogical characteristics of powdered sample (Mutaz and Dafalla 2014; Wang et al. 2019). The XRD analysis of GMZ07 bentonite in Fig. 5a signifies that GMZ bentonite contains 61% Mt, 26% quartz, 7% plagioclase and 6% feldspar (Xu 2019). The scanning electron microscopy (SEM) results performed on rough sodic GMZ bentonite in Fig. 5b suggest that the particles are spaced apart distantly from each other as pointed by arrows. The evolution of rough surfaces evidences the fractality characteristics in the Na- GMZ bentonite. The distribution of pore sizes determined by Barrett–Joyner–Halenda method is shown in Fig. 5c, where Na- GMZ bentonite has been categorized as mesoporous Liu et al. (2014). In addition, Transmission electron microscopy (TEM) performed by Xiang et al. (2019b) reveals that, the Mt particles are flaky and intact in the GMZ bentonite which shows smooth morphology without any corrosion at microstructural level (Fig. 5d). Considering the above-mentioned points regarding GMZ bentonite, initially, we discuss the thermal and hydromechanical characteristics of GMZ bentonite as compared with rest of the bentonites.

Hydro-mechanical characteristics of GMZ and other bentonites

The hydraulicity of the compacted GMZ bentonite and its mechanical characteristics have been studied in the recent past as shown in Figs. 5 and 6, respectively. The soil water retention curves (WRCs) of GMZ bentonite for unconfined and confined conditions and other prominent bentonites are also depicted in the plot between water content and suction (Fig. 6). It is important to state that, the negative pore water pressure refers to suction property. The WRC determines the capability of bentonite to hold moisture with change in suction value (Arifin et al. 2015; Villar et al. 2010). In Fig. 6, the WRCs for GMZ are plotted at room temperature (20 C) and at dry density of 1.7 g/cm^3 (Ye et al. 2010a). The water contents below 20% have higher suction values ranging from 6000 to 50,000 kPa for all given bentonites, whereas, for water contents greater than 40% the suction is logarithmically reduced between 800 kPa and 3000 kPa. Furthermore, at any given water content, the suction is minimum for Kunigel VI, while it is the highest for MX-80 bentonite. It is to say that, the ability of MX-80 to retain water is higher than that of Kunigel VI. Cui et al. (2008) attributed it to the presence of 79% and 46-49% Mt content in MX-80 and Kunigel VI, respectively. Moreover, Sun et al. (2014) determined the Soil water characteristics curve (SWCC) of highly compacted calcic GMZ at greater suctions (3 - 287 MPa) using the vapor equilibrium method. The SWCC explains the correlation among soils' moisture content (saturation degree and gravimetric moisture content) and suction, and it is considered as the key soil characteristics for evaluation of hydromechanical behavior, moisture movement. The effect of the SWCC on the stiffness and

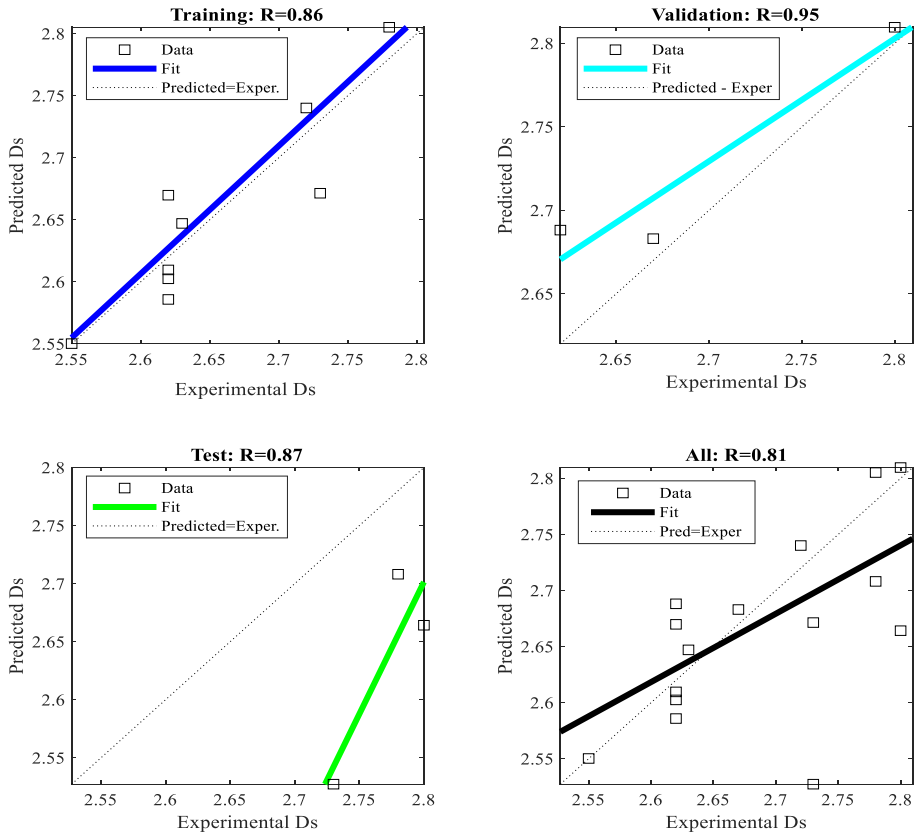

Data set	1	2	3	4	5	6	7	8	9	10	11	12	13	14	15	16
Experimental D_s	2.62	2.62	2.62	2.62	2.73	2.73	2.72	2.55	2.67	2.78	2.78	2.8	2.8	2.67	2.62	2.63
ANN D_s	2.65	2.65	2.65	2.63	2.69	2.72	2.84	2.59	2.70	2.77	2.79	2.77	2.83	2.80	2.66	2.71

Evaluation criterea	R^2	RMSE	MAE	NSE	RRMSE	P_i
	0.808	0.656	0.042	0.474	0.244	0.134

Fig. 3 Regression plot for evaluating surface fractal dimension (D_s) using ANN along with the respective values of performance indices for the predictive neural model

Table 2 Elemental composition of randomly selected global bentonites

S. No	Bentonite source/ name	Country	Elemental composition (% weight)										References
			SiO_2 (S)	Fe_2O_3 (F)	Al_2O_3 (A)	S+F+A	TiO_2	LOI	CaO	Na_2O	K_2O	MgO	
1	B75	Czechia	51.9	8.9	15.5	**76.3**	2.3	-	4.6	1.2	1.3	2.2	(Sun et al. 2019)
2	Kyeongju	Korea	56.8	6.0	20.0	**82.8**	0.8	-	2.6	1.3	0.9	0.8	(Lee et al. 2012)
3	GMZ	China	69.2	3.1	14.4	**86.7**	0.1	5.4	1.3	1.9	0.8	3.3	(Liu 2013)
4	VC-EL-COL4	Brazil	62.9	8.2	22.6	**93.7**	0.2	0.1	2.0	0.1	0.1	3.5	(Alves et al. 2016)
5	Ünye	Turkey	76.8	1.1	12.3	**90.2**	0.1	5.9	1.4	0.3	0.4	1.5	(Sakizci et al. 2010)
6	Egyptian Local	Egypt	54.9	9.3	17.0	**81.2**	1.5	8.1*	1.0	2.8	1.0	2.5	(Abdou et al. 2013)
7	Jordanian Raw	Jordan	60.9	6.5	13.0	**80.4**	1.1	-	1.2	2.9	3.0	3.1	(Al-Jariri and Khalili 2010)
8	Azzouzet	Morocco	53.4	-	17.3	**70.7**	-	14.2	1.7	1.0	0.3	3.7	(Er-ramly and Ider 2014)
9	Sardinia southern	Italy	59.4	2.4	18.9	**80.7**	0.2	11.1	0.9	1.0	0.5	5.5	(Cara et al. 2000)
10	Takhtbhai	Pakistan	53.1	9.1	12.4	**74.6**	1.0	6.1	12.9	0.0	2.5	2.6	(Afzal et al. 2014)
11	Lygumai	Lithuania	49.5	3.7	30.1	**83.3**	0.9	10.8	0.2	0.2	3.9	1.1	(Kiipli et al. 2008)
12	Grötlingbo	Sweden	50.8	2.0	26.7	**79.5**	0.4	10.5	0.9	0.5	5.4	3.2	(Kiipli et al. 2008)
13	Ruhnu	Estonia	55.1	1.7	24.5	**81.3**	0.3	7.3	0.4	0.7	6.3	3.6	(Kiipli et al. 2008)
14	Cape Mine	South Africa	65.9	3.6	15.3	**84.8**	0.5	5.1	1.1	2.7	1.1	3.1	(Masindi et al. 2015)
15	ThuanHai clay	Veitnam	62.6	3.0	16.7	**82.3**	-	-	2.1	2.4	0.6	1.9	(Thuc et al. 2010)
16	Ardestan mine †	Iran	56.4		14.3	**70.7**		17.0		4.1			(Faghihian and Godazandeha 2009)
17	Maghian clay	Algeria	70.3	2.6	12.3	**85.2**	0.2	-	1.7	1.9	2.4	1.5	(Angar et al. 2017)
18	BRS-291	UK	53.1	2.4	27.4	**82.9**	0.5	5.9	0.4	0.4	7.2	2.6	(Huff et al. 1993)
19	Chioarului	Romania	73.2	1.2	14.2	**88.6**	0.4	-	0.8	2.7	1.0	2.2	(Komlósi et al. 2007)
20	Tango	Nigeria	49.9	5.1	15.0	**70.0**	-	-	1.2	-	1.8	-	(Abdullahi and Audu 2017)
21	Wyoming	USA	55.4	3.0	20.1	**78.5**	0.1	14.7	0.5	3.8	0.6	2.5	Mahto and Sharma (2008)
22	Gujarat	India	59.4	12.8	15.0	**87.2**	1.3	5.7	1.7	1.2	0.1	3.1	Mahto and Sharma (2008)
23	KW-4	Japan	84.5	2.8	5.7	**93.0**	0.1	3.3	0.6	0.5	0.8	1.6	(Fukushi et al. 2010)
24	Miles	Australia	71.2	3.3	17.3	**91.8**	0.6	-	2.9	1.7	0.7	1.7	(Gates et al. 2002)
25	Puskwaskau	Canada	47.2	4.6	17.5	**69.3**	0.3	23.3	1.7	0.5	0.4	4.4	(Fanti 2009)

Note: LOI: loss on ignition, * at 1000 C, † Fe_2O_3, BaO, MgO, CaO, K_2O, SrO, ZnO, MnO, TiO_2 = 7.97%; If the combined percentage of the bold values exceed 70%, it is regarded as pozzolanic material by ASTM

strength characteristics of unsaturated soils is significant. Also, it is important for understanding soil-environment interactions, flow of water, solute transport processes, and could be employed for estimation of the hydraulic conductivity, shear strength and deformation of soils (Ye et al. 2019). On the other hand, for the compacted sodic GMZ bentonite, it was revealed that in low suction range (< 4 MPa), the confined specimens of soil caused relatively reduced water retention, whereas, at greater suctions (> 4 MPa) the confined and the unconfined specimens both yielded same water retention (Ye et al. 2014).

In suction versus water content graph, the WRCs are measured by using various concentrations of salt (S_0, S_1, S_2, S_3) and deionized water for the compacted GMZ bentonite (Fig. 6). S_0, S_1, S_2, and S_3 are the salt (NaCl) concentration/ bentonite ratio R_s (mmol/g) in each solution having values equaling 0, 0.101, 0.2014, and 0.310, respectively (He et al. 2019b). At a constant suction, the measured water content rises at high concentration of the pore fluid such that the rate of influence is directly related to suction (Ye et al. 2014). Equation 1 represents the modified model to explain the WRCs of heavily compacted GMZ bentonite while considering the effect of pore fluid concentration (He et al. 2019b). It is established that the predictions made by equations proposed by Fredlund and Xing (1994) better describe the SWCC and that this model shows good agreement among calculated values and measured data (Fig. 6).

$$\theta = C(\psi) \times \frac{\theta_s(c)}{\left\{ ln\left[e + (\psi / a(c))^{n(c)} \right] \right\}^m} \quad (1)$$

where θ is water content, C (ψ) is a correction function, ψ is the total suction, $\theta_s(c)$ is the saturated moisture content at

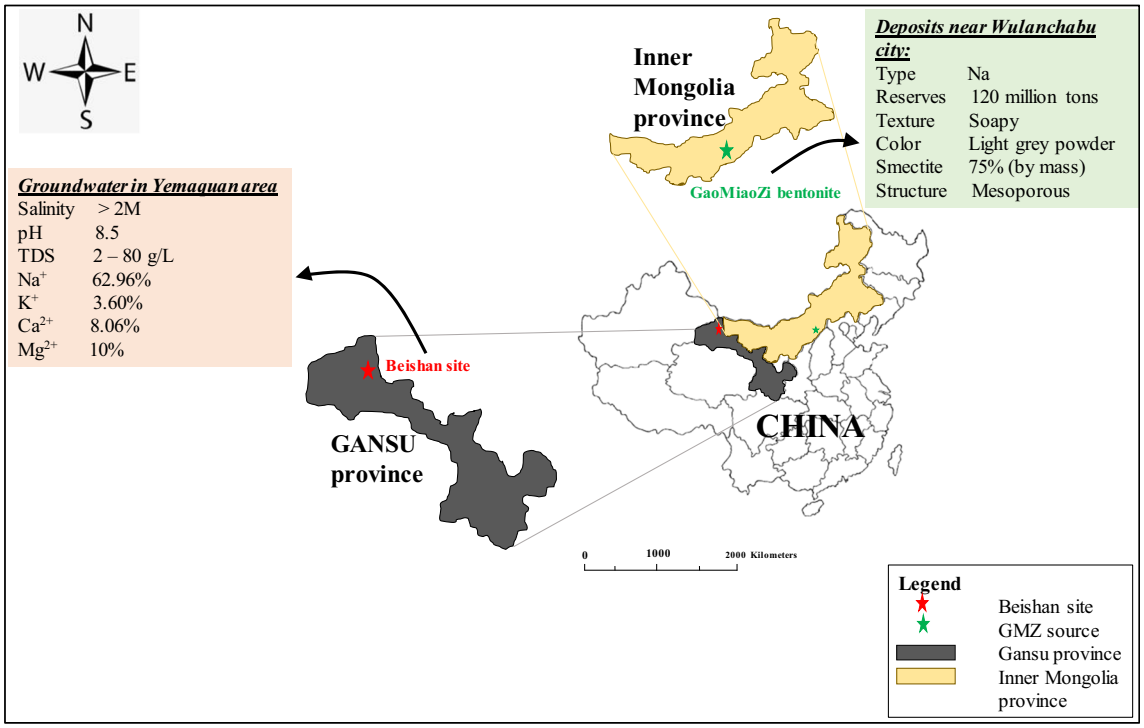

Fig. 4 Location and general features of Chinese GMZ bentonite deposits and geological repository site

existing chemical concentration, a(c) is the air entry value-related parameter (i.e., a) and the pore fluid chemical concentration, and n(c) is the slope value and pore fluid chemical concentration. Furthermore, Xu and Dong (2004) concluded that the water retention property can also be expressed by the fractal theory.

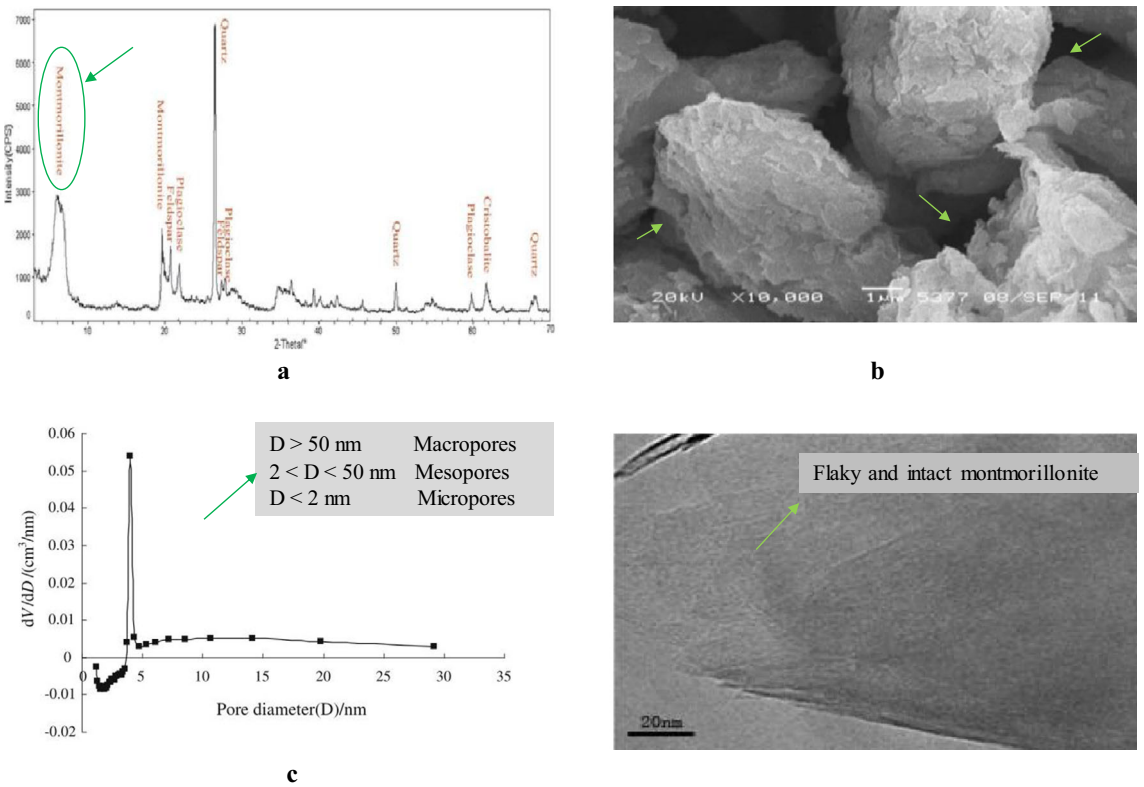

Fig. 5 Mineralogical and morphological characteristics of GMZ bentonite

Fig. 7 indicates the findings on P_s and permeability versus dry density obtained from the previous researches. The increase in dry density leads to higher P_s, larger unconfined compressive strength (UCS), and increased modulus of elasticity for all given bentonites thus depicting an exponential relationship (Liu 2013). GMZ bentonite with 15% water content is easily compactible to a more dense state in contrast to less than 10% or more than 20% water content. Wen and Jintoku (2005) found that, the UCS of GMZ bentonite with a water content near to optimum (ω=14%) is greater than the rest of the moisture contents. In addition, at higher dry densities (1.4 to 1.7 g/cm^3) the P_s is minimum for Kunigel VI while it is the highest for Febex bentonite. The degree of fluctuation in the GMZ bentonite ranges between the P_s curves of these two bentonites. A logarithmic relation is also obtained which correlates P_s and dry density of GMZ having regression coefficient of 93%. Zhang et al. (2019a) introduced a critical void ratio for highly compacted GMZ bentonite inundated with NaCl solution to demarcate the combined swelling due to double-layer swelling as well as crystalline swelling from that of only crystalline swelling. For specimens with a larger void ratio than this critical value, the P_s was inversely related to the concentration of NaCl solution because the double-layer swelling and crystalline swelling were inhibited. On the contrary, when these values are equivalent, the salt solution effects were almost negligible (Zhang et al. 2019a). It is noteworthy that P_s shows a nonlinear trend with time along with higher rate of increase in P_s obtained in early stages while attaining a straight horizontal line afterwards.

Additionally, the semi logarithmic plot of permeability and dry density reveals that increase in dry density of GMZ bentonite from 1.4 to 1.8 g/cm^3 reduces the permeability from 1×10^{-12} to 1×10^{-13} m/s, as shown in Fig. 7. Korean Ca-bentonite somehow follows the similar pattern at aforementioned range of dry density with decrease in hydraulic conductivity reported as $1x10^{-11}$ to $1x10^{-12}$ m/s. The range of dry density is between 0.2 and 1 g/cm^3 for other bentonites in accordance with the previous literature, wherein the reduction of permeability is several degrees higher than the compacted bentonites because of compaction. It is shown that hydraulic conductivity increases with the elevation of temperature, however, the hysteretic behavior in WRCs of highly compacted

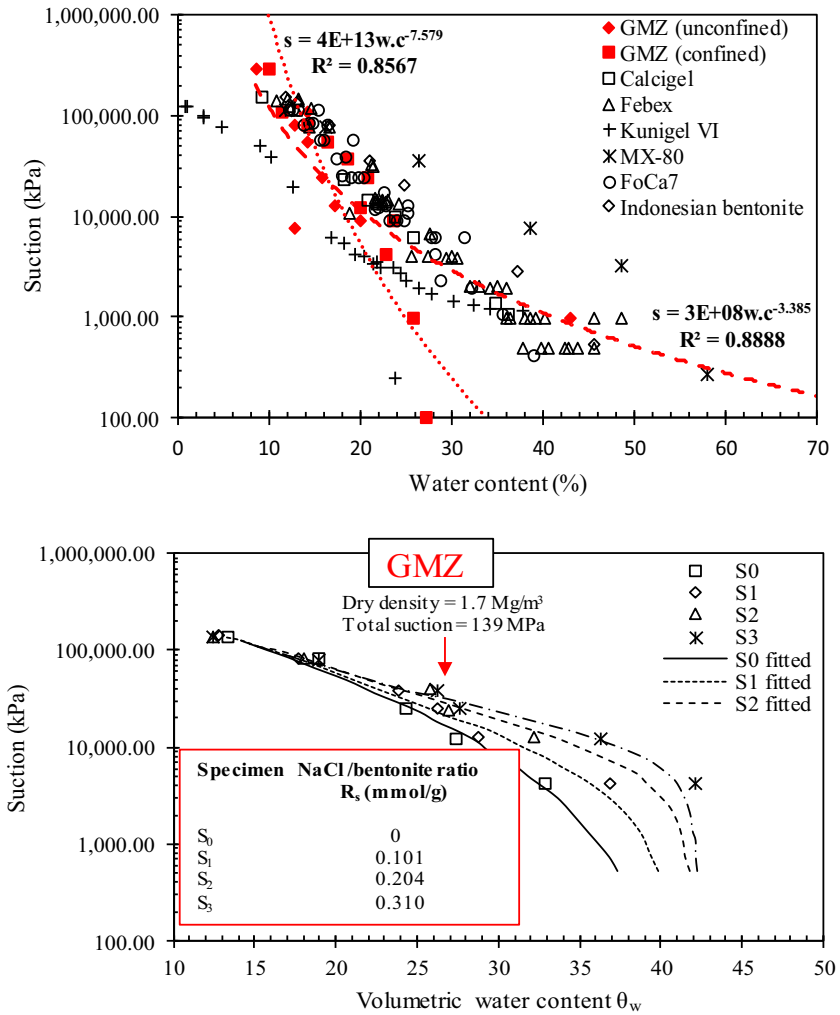

Fig. 6 Comparison of suction versus water content of GMZ bentonite and other global bentonites, with focus on soil water retention curves of GMZ bentonite inundated in saline solution, (Arifin et al. 2015; Komine 2004a; Mašín and Khalili 2015; Ye et al. 2010a)

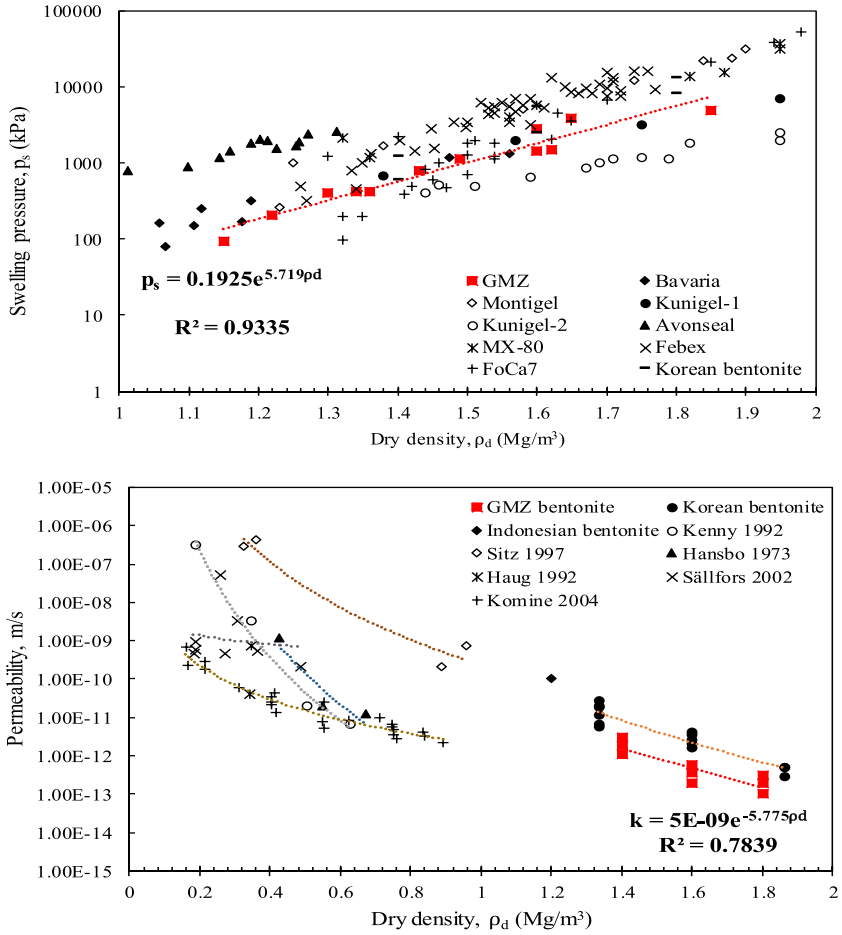

Fig. 7 Comparison of swell pressure and permeability behavior of bentonites with dry density for GMZ bentonite and other global bentonites, from past literature

GMZ bentonite exhibits minimal effect at 20 or 40 °C (Ye et al. 2010a). The modified equation based on fractal approach containing the effect of osmotic suction can well predict the hydraulic conductivity of unsaturated expansive clays. In addition, Ye et al. (2010a) reported that the unsaturated permeability of unconfined compacted GMZ bentonite is greater than that of the confined case which could be associated with microstructural changes at the time of hydration in confined case.

In Belgium, repositories were designed by analyzing clay that is based on multiple barrier system between the HLW and the biosphere. In 1980, decision was taken to build high activity disposal experimental facility (HADES) in Belgian Boom clay formation at 223 m depth for evaluating the feasibility of the disposal concepts. According to Xiangling et al. (2006), it aimed at providing reliable data on the performance of repository barriers. A large-scale long-term (8.5 years) experiment employing more than 500 sensors was conducted by designing full-scale thermal-hydro-mechanical (T-H-M) mock-up test for the HLW in Granite subjected to specified boundary conditions. The sensors were capable to bear mechanical stress, high temperature, and harsh environment. Major implications of the thermal aspects in the transport processes were yielded at the end of the experiment (Cui and Tang 2013; Martin et al. 2006). Also, an engineering-scale test facility (KENTEX) was constructed to validate the T-H-M behaviors in South Korea (Lee et al. 2006). Yet another large-scale heating test on FEBEX bentonite was conducted by subjecting to cooling and subsequent partial dismantling wherein all the conditions of an HLW repository were reproduced at full scale under realistic conditions. Important THM parameters, such as temperature, relative humidity, stresses, and fluid pressures, were determined in the EBS and nearby field rock. It was concluded that, the thermal field has a substantial effect on the hydration time, hydraulic gradient and rate of cooling. Also, the model predictions were in close agreement with the experimental results (Sánchez et al. 2012). Similarly, in China, a large-scale mock-up facility was made in the Beijing Research Institute of Uranium Geology (BRIUG) which comprised a heater for simulating a container of radioactive waste and was kept in the compacted GMZ-Na-bentonite blocks and pellets. According to Chen et al. (2012), the model of Alonso-Gens was employed to generate the mechanical behavior of the BBMs under unsaturated conditions. It was revealed that the temperature distribution is affected by the thermal conductivity that rises with the increasing saturation percentage and the specific heat of

bentonite. Additionally, Liu et al. (2014) explained that the stress evolution in the GMZ buffer material was observed to be affected by the gravity, thermal expansion at elevated temperature, and the P_s generated by water penetration.

The summary of obtained correlations and their studied ranges in Figs. 6 and 7 are tabulated in Table 3, which suggests that the regression coefficient values are higher except for the relationship between coefficient of hydraulic conductivity and dry density that falls below 80% (Gueddouda et al. 2016). All other relationships have R^2 values above 86% that corroborates the previous findings.

Fractality characteristics of GMZ and other bentonites

A number of researchers have conducted research in the field of fractal geometry (FG) since 1990 owing to the promising characteristics and cutting-edge application to research undertaken today. According to Mandelbrot (1983), FG helps in describing the surface texture since Euclidean geometry exhibit four topological dimensions. According to Gareche et al. (2016), the rheological measurements indicate that particles of highly expansive clays such as bentonite are structured in a fractal network. Furthermore, the fractal approach efficaciously describes the solid-pore-fracture geometry of coal and quantifies its porous structure and helps to understand the surface roughness and methane (CH_4) storage capacity of a coal reservoir (Liu and Nie 2016; Wang et al. 2019).

A number of researchers have published articles related to the SFD or D_s of GMZ bentonites (Xiang et al. 2014a; Xu 2003; Xu et al. 2004), its calculation and effect on swelling characteristics of geological repository (Liu et al. 2014; Xiang et al. 2014b; Xu and Dong 2004; Xu et al. 2004), the role and calculation of osmotic suction in determining D_s value (Li et al. 2019; Li et al. ; Xiang et al. 2015), and the calculation of peak shear strength of saline solution inundating the GMZ (Xu 2019), among others. In the following, the role of osmotic suction, methods of calculating surface fractal dimension, and effect on volume change and strength properties will be scrutinized in relation to fractality of bentonites-based materials with focus on GMZ bentonite. A short summary of the methodologies used along with the derived models are presented in Table 4. It can be seen from Table 4, that the SFD of GMZ bentonite can be found from NAIT results and it is directly related to amount of clay fraction. While, it is inversely proportional to NaCl solution concentration. The swelling characteristics decreases while the strains decline with increasing salt concentration. The results obtained for the D_s from swelling deformation agree with those from NAIT results. The determination of P_s of GMZ bentonite is better explained by fractal model since the DDL theory underestimates the P_s values. Moreover, the disintegration of Mt particles upon corrosion led to a more uneven surface and thus D_s rises significantly. However, in the absence of saline solutions, the effect of osmotic suction will be no more thus limiting the applicability of fractality characteristics of the GMZ bentonite.

Implications and limitations of fractal approach

In 1988, the fractal theory was firstly introduced by Dexter regarding soil structure. Such theories are applicable to explain the processes of water retention and movement in soils (Young et al. 2001), because the solid phase of different natural porous materials exhibit fractal behavior (Tyler and Wheatcraft 1992). Perfect and Kay (1995) concluded that fractals are applied as a powerful tool in case of expansive clays to explain their physical properties (grain and pore size distribution, bulk density, pore surface area, and microtopography) and physical processes (diffusion, adsorption, water and solutes transportation, and fragmentation). Usually, the D_s of grain size distributions of clays are increased with the clay fraction content and, thus, the adhesion and frictional force are increased subsequently (Ren et al. 2001). Also, the fractal dimensions of the pore structures can be used to quantitatively describe the complexity of pore structures (Guo et al. 2012). The D_s of soil pores is independent of the compaction and the net normal stress, and remains constant for various combinations of compaction and the normal stress. Furthermore, it has an obvious physical meaning, so it is beneficial in regards to the empirical parameters of the SWCC. Correlations between the D_s and the compression curve, hydraulic characteristics, soil cohesion and swelling

Table 3 Summary of correlations obtained for hydromechanical behavior of GMZ bentonite (from past data)

No.	Relationship	Correlation based on past data	Remarks	R^2
1	Swell pressure ~ dry density	$p_s = 0.19e^{5.72\rho_d}$	P_s range: 93–4887 kPa	0.93
2	Hydraulic conductivity ~ dry density	$k = 5 \times 10^{-9}e^{-5.775\rho_d}$	k range: 1×10^{-10}–3×10^{-13} m/s	0.78
3	Suction ~ water content *	$s=3\times10^{8}w^{-3.385}$	s range: 900–350,000 kPa	0.88
4	Suction ~ water content †	$s=4\times10^{13}w^{-7.579}$	s range: 100–350,000 kPa	0.86

Note: * unconfined GMZ, † confined GMZ

Table 4 Previous literature (2000 to 2020) on fractality characteristics of Chinese GMZ bentonite-based materials (↑ represents increase and ↓represents decrease)

No.	Reference	Bentonite material	Type	Characteristics examined	Key findings
1	(Zhang 2002)	bentonite and bentonite–polymer muds	Commercial	Fractality of granularity distribution data	• The inhomogeneity in granularity distributions are effectively and quantitatively explained using the fractal dimensions. • For aqueous bentonite muds Ds ↑ as clay content ↑. In addition, D_s ↓ with ↑ NaCl content. • T= 28–180 °C, D_s exhibits slight changes, whereas, at higher temperature the D_s ↑ greatly.
2	(Xu 2003)	GMZ	Na-type	D_s of swelling clay minerals	• Swelling deformation and P_s are directly related to amount of water volume absorbed, which is related the surface fractality of bentonite. • D_s of swelling clay minerals is estimated by: $\frac{V_W}{V_M} = K_{swell} P^{D_s-3}$ • D_s of Wyoming bentonite (i.e. 2.64) from the swelling tests is identical to the one by the N_2 adsorption method. However, this D_s is greater than that obtained by MIP.
3	(Jiang et al. 2014)	GMZ	Na-type	DDL ~ fractal theory	• DDL and fractal theories are explained on comparative basis. **1/K** = Double layer thickness (cm), **D** = dielectric constant, **k** = Boltzmann constant, η_0 = bulk solution electrolyte concentration, ε = unit electrolyte charge, **v** = cation valence, **T**= absolute temperature $^{*}\frac{1}{K} = \sqrt{\frac{DkT}{8\pi\eta_0\varepsilon^2\nu^2}}$: • Effect of electrolyte concentration on P_s is not explained quantitatively by DDL and the predicted P_s is lower than the experimental data at lower swelling strain. • There is lack of method to determine K so both theories are merged while proposing a new prediction method.
4	(Xiang et al. 2014b)	GMZ	Ca-type	D_s , swell deformation	• D_s was determined from swelling deformation test that was also confirmed by N_2 isotherm test. Values from both tests were identical. • D_s is also helpful in estimation of swelling deformation, when swelling coefficient K of montmorillonite is determined using the DDL model.
5	(Xu 2018)	GMZ	Na-type	Relation between Ψ~w_c of bentonites	• Correlation of total suction versus water content can be expressed by a power-law function having exponent D_s–3. • $w = a\psi^{D_s-3}$, $w = ap_s{}^{D_s-3}$, $w = \frac{C_m\rho_w}{\rho_m}\frac{V_w}{V_m}$, $p_s = \frac{RT}{M_W V_{W0}}\left[ln\left(\frac{P}{P_0}\right)\right]$ • D_s is determined using N_2 adsorption technique. Satisfactory agreement of the relation with the experimental data has been attained. • Alternate and reliable method for determining D_s.
6	(Xiang et al. 2019a)	GMZ	Na-type	Swelling properties of compacted bentonite in NaCl and $CaCl_2$	• Swelling characteristics ↓ with salt concentration ↑. Swelling strains in NaCl solution were relatively ↑. • D_s was measured using N_2 adsorption and swelling fractal model was used to predict modified effective stress. • Swelling coefficient K was also considered for explaining swell due to exchangeable cations. DDL used to calculate K (good prediction for Na-bentonite in dilute solutions in contrast to that for Ca-bentonite).
7	(Xiang et al. 2019b)	GMZ	Na-type and Ca-type	Effect on D_s by corrosion	• D_s tends to ↑ as the corrosion process progresses. • ↓ in Mt had no specific relation with D_s that was also confirmed by swelling deformation tests. • Swelling characteristics was defined by a unique e_m–p_s relationship with a same D_s value. • From SEM and TEM, the disintegration of Mt particles upon corrosion led to more uneven surface and thus D_s ↑.
8	(Li and Xu 2020)	GMZ	commercial	calculation of modified effective stress related to π of saline solutions	• π were achieved using the calculated ϕ and two filter paper techniques were conducted for verification purposes. • Microscopic and macroscopic aspects of the clay behavior in salt solutions were described and quantified using modified effective stress concept.

Note: * Poisson-Boltzmann equation is applicable for large monovalent ions only (Barbour and Fredlund 1989)

MIP mercury intrusion porosimetry, e_m void ratio of Mt., p_s: vertical stress

properties are already available (Kravchenko and Zhang 1998; Xu 2004). Tao et al. (2019) used the fractal theory to estimate the unsaturated hydraulic conductivity of Hunan clay with different initial void ratios in order to characterize its structure

in contrast to the tedious conventional methods of integral and sectional calculation. Hence, time was saved and accuracy was achieved as the measured and the predicted values were found in close agreement with each other. Substantial linear relationships existed between D_s and, clay content, silt content, fine sand and the soil porosity. Except the sand content, positive correlations with the fractal dimension were obtained for other parameters (Liu et al. 2009).

The limitations associated with modelling via fractal approach are important to better estimate the desired parameters. Perfect and Kay (1995) stated that, when the fractal algorithms were applied to estimate the SWCC, discrepancies in selection of type of algorithm arises that leads to erroneous and limited implications of the fractal model. In many fractal models which incorporated the concept of the Von Koch curve represented only the pore-solid interface thus limiting their use to model the resultant clay structure. However, mass fractals exhibit an improved performance in the sense that they closely associate the solid and pore phases (Perrier et al. 1999). Furthermore, the morphology of clay structure is fractal within some scale limits, however, there is a need of further research to understand the relationship among fractal dimensions of the expansive clays structure. As a result, fractal models with contrasting assumptions were employed by Gimenez et al. (1997) for the estimation of soil hydraulic characteristics. The molecular D_s of soil particle surfaces is also a significant parameter that affects soil adhesion. Ren et al. (2001) concluded that it is directly related to SSA and soil adhesion, and its relation with the D_s is still not clear. Also, the interpretation of the power-law parameters is complex which are obtained by performing fractal analysis. Variety of researchers take the observation of a power-law in a clay process as evidence of fractal nature implying that the process follows power-law behavior. But fractal processes do comprise power-laws that are not synonymous with fractals. Thus, research is in progress in this area and it is expected to continue in coming years (Young et al. 2001).

Role of osmotic suction

In the presence of a saline solution, the osmotic component is reported to significantly affect the swell parameters and strength of bentonite or bentonite-sand mixture in the design of geological repository for the disposal of HLW (Arifin and Schanz 2009; DI MAIOĆ 1996; Li and Xu 2020; Rao et al. 2013; Schanz and Al-Badran 2014). When the clay containing distilled water is immersed in a saline solution, the interparticle forces are believed to control the initial clay structure and the clay volume may experience changes due to chemical and osmotic consolidations, which are results of changes in the concentration of ions and osmotic pressure, respectively (Mitchell and Soga 2005). A summary of governing equations used for calculation of swelling characteristics of highly compacted expansive clays incorporating the effect of osmotic suction in the viewpoint of surface fractality are listed in Table 5.

Methods of calculating D_s

Fig. 8a and b shows the methods of determining the SFD of both calcic and sodic GMZ bentonites using N_2 adsorption test (Xiang et al. 2014a) and swell deformation test (Xu et al. 2014), respectively. Avnir and Jaroniec (1989) proposed an easy-to-use method to find the D_s from the N_2 adsorption method using Frenkel−Halsey−Hill (FHH) theory. According to the FHH theory, the volume of nitrogen adsorbed by bentonite powder V_{ads} bears a relationship with the relative air pressure P_0 / P (Li et al. 2019; Xu 2018). Furthermore, other methods have been used in the literature for determination of D_s; X-ray CT imaging (Wang et al. 2019), SAXS (Peng et al. 2020), X-ray computed tomography (Gouze et al. 2003; Zeng et al. 1996), SEM image analysis (using a box-counting method) and electrochemical impedance spectroscopy methods (Lü et al. 2019; Risović et al. 2008), mercury intrusion porosimetry (MIP) (Zeng et al. 2010) among others. Of these, SAXS has been the most commonly employed technique (Peng et al. 2020).

The fractal dimension values of Na-GMZ are 2.66 and 2.72 whereas that of Ca-GMZ are 2.80 and 2.84, by nitrogen adsorption isotherm technique, NAIT, (analyzed using FHH) and swell deformation method, respectively (Xiang et al. 2014b). It is found that for low Na^+, the D_s has higher value while for high Na^+ the D_s drops down (Xiang et al. 2015). In NAIT, the hysteresis loop between adsorption and desorption isotherm (Type IV isotherm) shown in Fig. 8a provides an insight about slit-shaped mesoporous structure of bentonite. In the N_2 adsorption technique, Pfeifer and Cole (1990) found that the interface is governed by liquid-gas surface tension, which means that capillary condensation is dominant instead of adsorption. According to Xiang et al. (2019a), the global adsorption process suggests $P/P_0 = 0.01$ to 0.99 for estimation of D_s. Moreover, it is recommended as highly accurate method to determine D_s by Xiang et al. (2014b). However, Lü et al. (2019) concluded that increasing D_s tends to lower the compression strength but it enhances the permeability characteristics.

Xu et al. (2014) calculated the D_s of various Mts by using Equation 2 which incorporates fractal approach (Fig. 9).

$$\frac{V_W}{V_c} = KP_s^{D_s-3} \tag{2}$$

The range of selected Mt ranges from 2.38 to 2.82. As mentioned earlier, the lower value indicates smooth surface while the higher value suggests that surface is rough. The D_s values of GMZ, Febex and Foca7 are 2.78, 2.80, and 2.82, respectively. The void ratio is plotted against P_s values over

Table 5 Summary of governing equations in swelling characteristics of highly compacted expansive clays incorporating the effect of osmotic suction in viewpoint of surface fractality

	Governing equation	Remarks	References
1. Concept of fractals	(a) $property \propto scale^{-D}$ (b) Hausdorff measure, $H_{\delta}^{S}(F)$ $H_{\delta}^{S}(F) = inf\left\{\sum_i |U_i| : \{U_i\}\right\}, \{U_i\}$ is a δ- cover of F (c) Hausdorff dimension, D_H Therefore, at $F \subseteq R_n$, the Hausdorff dimension equals: $D_H = inf\{s : H^{\delta}(F)=0\} = sup\{s : H^{\delta}(F)=\infty\}$	• The exponent D is defined as the fractal dimension of the object while the scale is a characteristic measure of the disorderly object. • Fractal geometry can be defined by $H^{s}{}_{\delta}(F)$ and D_H at various levels of magnification. • In this regard, fractal is defined as: If D_H (a fraction) of a set in n-dimensional Euclidean space R_n exceeds the topological dimension then that set is known as 'fractal set' or simply 'fractal'. • Examples of common fractals are Koch curve, Koch snowflake, Sierpinski triangle, and Cantor set among others.	(Avnir and Jaroniec 1989; Chen et al. 2016; Fernández-Martínez et al. 2019; Zhang 2002)
2. Modified effective stress (p')	(a) Modified effective stress equation (by Sridharan): $\overline{C} = \overline{\sigma} a_m = \sigma - \overline{u}_a - R + A$ (b) Hamaker's equation: $F = \frac{A}{6\pi d^3}$, (where F is force in dyne/cm^2) (c) Modified effective stress equation (by Rao and Thyagaraj): $p' = \sigma - u_a + \alpha\Delta\pi$, where α is osmotic efficiency. (d) Modified effective stress equation (by Xu): $p' = (p - u_a) + p_{\pi}$ $p_{\pi} = \pi\left(\frac{p}{\pi}\right)^{D_s - 2}$ $p' = p + \sum_{i=1}^{n} \pi_i \left(\frac{p}{\pi_i}\right)^{D_S - 2}$ (e) Peak shear strength of bentonite $\tau_f = c' + p' \tan\varphi'$	• In the modified effective stress equation incorporating osmotic suction the IP electrical attractive and repulsive forces are considered. • Repulsive forces assist in supporting the external loads and are generated due to coulomb repulsion and osmotic forces (DDL forces, in particular). The attractive forces, which tend to reduce the volume of specimen, are due to the weak van der Waals forces. • Rao and Thyagaraj proposed, $p_{\pi} = \beta\pi$ with β value in the range of 0 to 1, which is still difficult to determine. • The surface of bentonite is characterized by peak shear strength and accordingly a fractal model is developed for bentonite surface. • Using Mohr-Coulomb criterion, the peak shear strength for GMZ bentonite treated with saline solution has been explained theoretically with the aid of modified effective stress. • The shear strength of compacted weak expansive clay treated using NaCl having concentration (0.5 and 1 mol/L) reduces.	(Rao and Thyagaraj 2007; Sridharan and Venkatappa Rao 1979; Xi et al. 2015; Xiang et al. 2017; Xu and Liu 1999; Yu et al. 2019)
3. Osmotic suction (π) determination	(a) Total suction = Matric suction + Osmotic suction $h_t = h_m + h_{\pi}$ or $\psi = -(u_a - u_w) + \pi$ $h_t = \frac{RT}{V} ln\left(\frac{P}{P_0}\right) = 137182 ln\left(\frac{P}{P_0}\right)$ (at 25 °C)	• The swell pressure of bentonite is equal to sum of matric and osmotic components of the total suction. • Osmotic suction in bentonites is due to the dissolved salt (or ion or solute) concentration in the pore water, whereas, matric suction is due to the capillary and the sorptive forces and the adsorption of solid surfaces.	(Arifin and Schanz 2009; Bulut et al. 2001; Mašín and Khalili 2015; Mokni et al. 2014; Rao et al. 2013; Thyagaraj and Salini 2015; Zhang et al. 2020)
	(b) Van't Hoff equation $h_{\pi} = \pi = -\boldsymbol{\nu RT\phi}$ $\pi = RT(C_c - 2C_0)$ (c) Osmotic suction for dilute solution $\pi = \frac{RTx_b}{V_{m,A}^*} \sim \frac{RTn_b}{n_a V_{m,A}^*} = RTc_{B'}$	• The osmotic suction of saline solution is determined by considering valence of interlayer cation, the universal gas constant, the absolute temperature and molar concentration of salt solution. • $C_c < C_0$ ➔ crystalline swelling only, $C_c > C_0$ ➔ osmotic swelling occurs. C_c: cations concentration (mol/L) at mid of clay platelets, C_0: cations concertation (mol/L) in bulk solution.	(Avnir and Jaroniec 1989; Li and Xu 2020; Mokni et al. 2014; Rao et al. 2013; Watt-Smith et al. 2005; Xu 2018)
	(d) Lang's equation (1967) $\phi = \frac{\rho_w}{vmw} ln\left(\frac{P}{P_0}\right) T$	• It is used to determine osmotic coefficient considering unit weight, specific volume, molecular mass of water and the water vapor pressure.	(Lang 1967)
	(e) Simplified Debye-Hückel (SDH) equation by Pitzer and Mayagora $\phi = \lvert v_c v_a \rvert f + c\left(\frac{2n_c n_a}{\zeta}\right) B_{MX} + c^2 \frac{2(n_c n_a)^{3/2}}{\zeta} C_{MX} + 1$ $B_{MX} = \beta_{MX}{}^{(0)} + \beta_{MX}{}^{(1)} e^{-\alpha I^{1/2}}$ $f = -d \frac{I^{1/2}}{1 + 1.2 I^{1/2}}$ (f) Osmotic coefficients obtained by deriving G^{ex} $\phi - 1 = -\frac{\partial G^{ex} / \partial n_w}{RT \sum_i ci}$	• The osmotic coefficient calculation is complex due to saturated vapor pressure dependence upon solute type and concentration, so, this equation is derived to ultimately determine osmotic suction. • ζ is the number of ions that the solute can dissociate in solution (e.g., NaCl = 2), where $\beta_{MX}{}^{(0)}$ and $\beta_{MX}{}^{(1)}$ are empirical parameters. I is referred to as the ionic strength. • SDH is suitable for aqueous solutions having monovalent ions.	(Li and Xu 2020; Li et al. 2019; Li et al.)

Table 5 (continued)

	Governing equation	Remarks	References
4. Surface fractal dimension (D_s)	(a) By Frenkel–Halsey–Hill (FHH) Model $S(r) - C_a r^{2-D}$ $S = (RT/\gamma)\int_V^{V_{max}} ln(p/p_0)\mathrm{d}V$ $r = -2\gamma V_m/[RTln(p/p_0)]$ $lnV_{ads} = C + (3-D_s)ln\left[ln\left(\frac{p_0}{p}\right)\right]$	• According to the FHH equation, the adsorbed nitrogen by bentonite and the corresponding relative air pressure are interrelated. • The molecular diameter of N_2 and hydrone resembles so it is suitable to describe the water imbibing by FHH equation. • The D_s of Tsukinuno (Japan), commercial (China) and GMZ calcium bentonites are 2.66, 2.65 and 2.78, respectively.	(Li et al. 2019; Mahamud and García 2018; Mendhe et al. 2017; Tripathy et al. 2019; Watt-Smith et al. 2005; Xiang et al. 2014a; Xiang et al. 2014b; Xu 2019; Zeng et al. 2013; Zhang et al. 2014)
	(b) By Swell deformation test $e_m = \frac{V_W}{V_M} = KP_e^{D-3}$ where, $K = e_m P_e^{3-D_s}$ $e = \frac{V_V}{V_S} = \frac{V_W}{V_S} = \frac{C_m V_W}{V_M} = C_m e_c$	• D_s is also calculated by swell deformation test undertaken in laboratory. The D_s of 36 Na-Mts range from 2.44 to 2.72. • The void ratio of montmorillonite is plotted on the ordinate and the effective stress incorporating osmotic suction on abscissa on log-log plot. • As in DDL model, the vertical overburden pressure must be equal to net interactive force between Mt layers, so, $P_e = f_{repulsive} - f_{attractive}$ (Guoy Chapman & Hamakers's equ used). • D_s obtained from swelling deformation are similar to that of FHH equation. So, it is a reliable method for determining D_s.	(Agus and Schanz 2008; Xiang et al. 2014a; Xiang et al. 2017; Xu and Lacidogna 2011; Xu 2003; Xu 2018)
	(c) By Neimark model in the form of Kiselev and Kelvin equation: $A \propto r^{2-D}$ $A = (RT/\gamma)\int_{V_{ads}}^{V_{max}} ln(p/p_0)\mathrm{d}V$ $r = -2\gamma V_m/[RTln(p/p_0)]$	• Unlike the FHH model, which is based on multilayer adsorption, it employs model independent method. • D_s from Neimark model are smaller than obtained by FHH because surface is characterized by larger pores (r > 2nm) where capillary condensation occurs.	(Jaroniec 1995; Xiang et al. 2014b)
	(d) By Freundlich isotherm model method $Q_e = K_F C_e^n$ $N = D_s - 2$ Note: The Freundlich isotherm of Pb (II) ion adsorption on the Na- GMZ bentonite has; 1/n = 0.3921, K_F = 4.9317	• Freundlich isotherm model yields smaller D_s values than the FHH isotherm model. • The latter is comparatively accurate and complex as the liquid-phase adsorption involves greater complications as compared with vapor-phase adsorption. • D_s is determined by Small-angle X-ray scattering (SAXS), adsorption-, nuclear magnetic resonance (NMR)-based methods, and Transmission electron microscopy (TEM).	(Liu et al. 2014; Lv et al. 2020; Malekani et al. 1996; Matusewicz et al. 2013; Xu et al. 2020)

log-log plot and the slope of power function of the fitted line is D_s-3 (Fig. 9). Note that the D_s of Mt from Alaska has been calculated as 2.625 using Eq. 2 based on swell deformation data for the sake of clarifying the calculations.

Fig. 10(a) depicts that D_s increases with the increase in Mt content in sodic bentonite whereas it decreases in the case of higher Mt content for calcic bentonite (Xiang et al. 2014b; Xiang et al. 2015; Xu 2018; Xu et al. 2004; Xu et al. 2014). The swelling coefficient β or K in the Eq. 2 increases as the D_s value drops (Li et al.). Although the swelling coefficient and SFD of GMZ bentonite are both instinct physical properties of bentonite, they can be correlated in the form of Eq. 3 as below;

$$D_s = 3.14\mathrm{K}^{-0.056} \quad (3)$$

Secondly, Fig. 10(b) shows that D_s increases with salinity (up to 3 g/L NaCl) whereas it decreases afterwards. Peng et al. (2020) concluded that higher amount of NaCl will bring about higher deterioration in the surface morphology thus attaining a greater D_s value (ranging from 2.44 to 2.51). It is to say that, the structure of compacted silty soil is largely governed by the salinity of pore water, however, according to the findings of Leong and Abuel-Naga (2018), the shear strength remained unaffected due to the development of osmotic suction or the osmotic gradient. Moreover, with increase in average pore size of the bentonite particles the D_s undergoes a slight reduction from 2.7 to 2.5.

Effect on volume change and strength properties

At a total vertical pressure to P_s ratio of less than unity, when the osmotic suction in pore water increases it acts as an additional total stress component which leads to lowering the swelling potential of the compacted clay specimens (Rao and Thyagaraj 2007; Xu et al. 2014). Therefore, the modified effective stress denoted by p^e is related to the osmotic suction and effective stress is modified by added osmotic suction component to the vertical pressure in compacted bentonite.

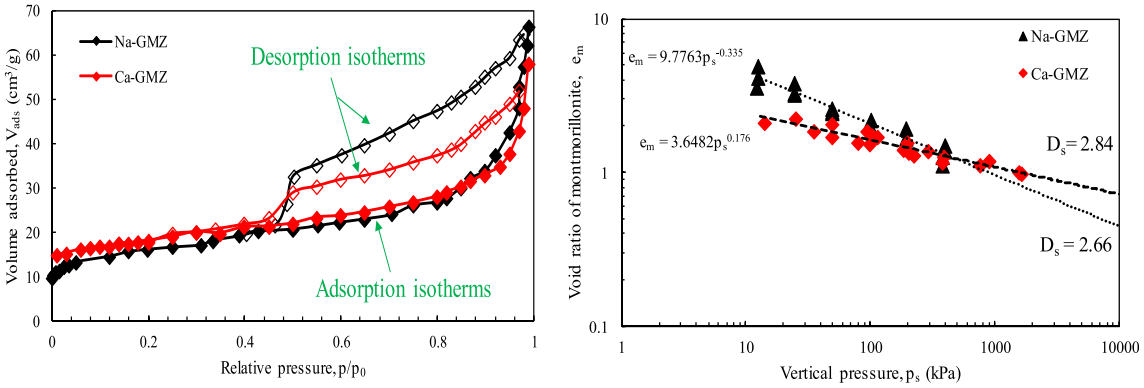

a. Nitrogen adsorption isotherm test results **b.** Swell deformation test results

Fig. 8 Method of determining D_s of GaoMiaoZi bentonite by N_2 adsorption technique and oedometer test

The p^e incorporating with osmotic suction can be expressed in the form of Eq. 4. According to the Mohr-Coulomb criterion, the peak shear strength of bentonite saturated by saline solution is expressed in Equation 5 (Xu 2019):

$$P^e = p' = p + p_\pi = p + \sum_{i=1}^{n} \pi_i \left(\frac{p}{\pi_i}\right)^{D^S - 2} \tag{4}$$

$$\tau_f = c' + p' tan\varphi' \tag{5}$$

where, P^e or P' is the modified effective stress incorporating effect of osmotic suction, p is effective stress, π is the osmotic suction, D_s is the surface fractal dimension, τ_f is shear strength, c' is effective cohesion, and φ' is the effective angle of internal friction.

The shear strength of GMZ07 bentonite was plotted against conventional effective stress and the modified effective stress incorporating osmotic suction. In addition, the comparison of direct shear test results data obtained from Fang et al. (2019) and Xu (2019), respectively, was done which is visualized in Fig. 11. The shear strength at constant conventional effective stress are recorded to increase with increasing dosages of NaCl concentration in both cases (Fig. 11a). On the other hand, in the plot of shear strength versus modified effective stress in Fig. 11b, the data by Xu (2019) has been replotted here (using Eqs. 4 and 5) that followed a unique line in τ_f - p′ plane while yielding an effective cohesion equaling 118 kPa and the internal friction angle of 12.82 . The data by Fang et al. (2019) was also replotted similarly, and since it had a large

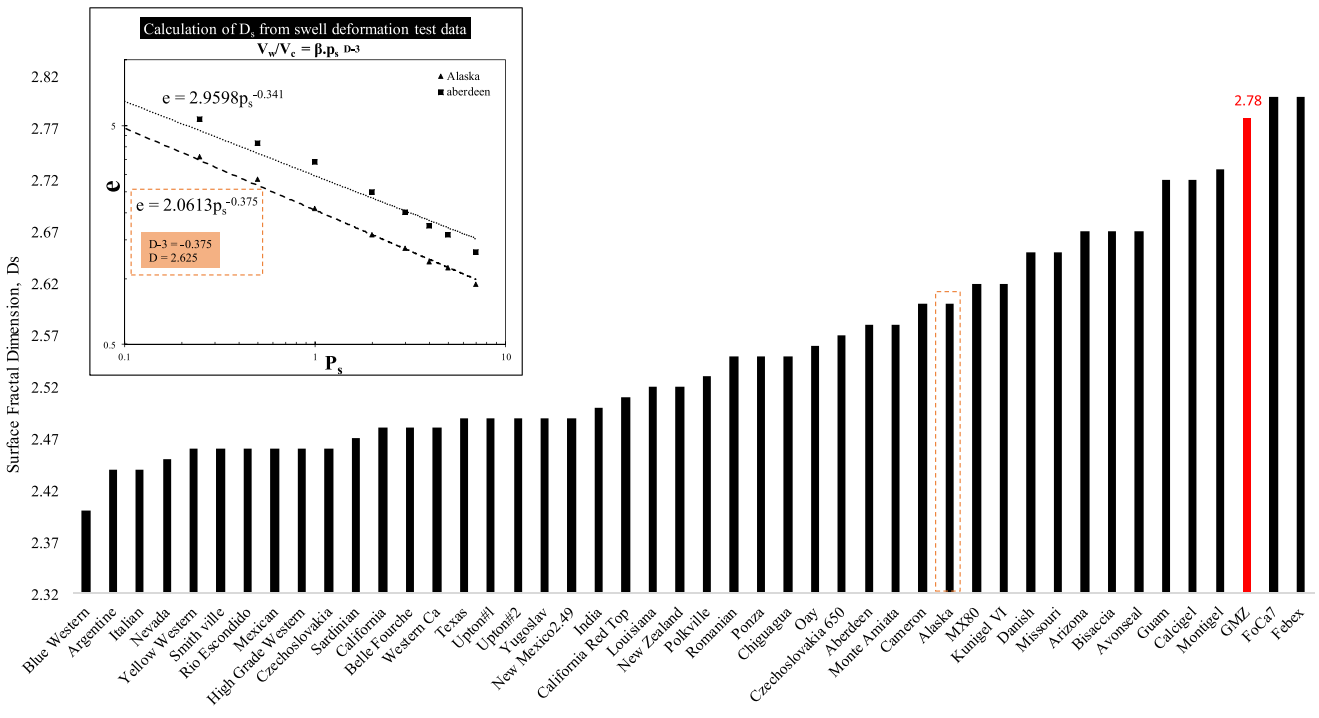

470

Fig. 9 Surface fractal dimension (D_s) of variety of bentonites across the world, calculated using fractal approach, Data from (Li et al. 2019; Low 1980; Xu 2018; Xu et al. 2014)

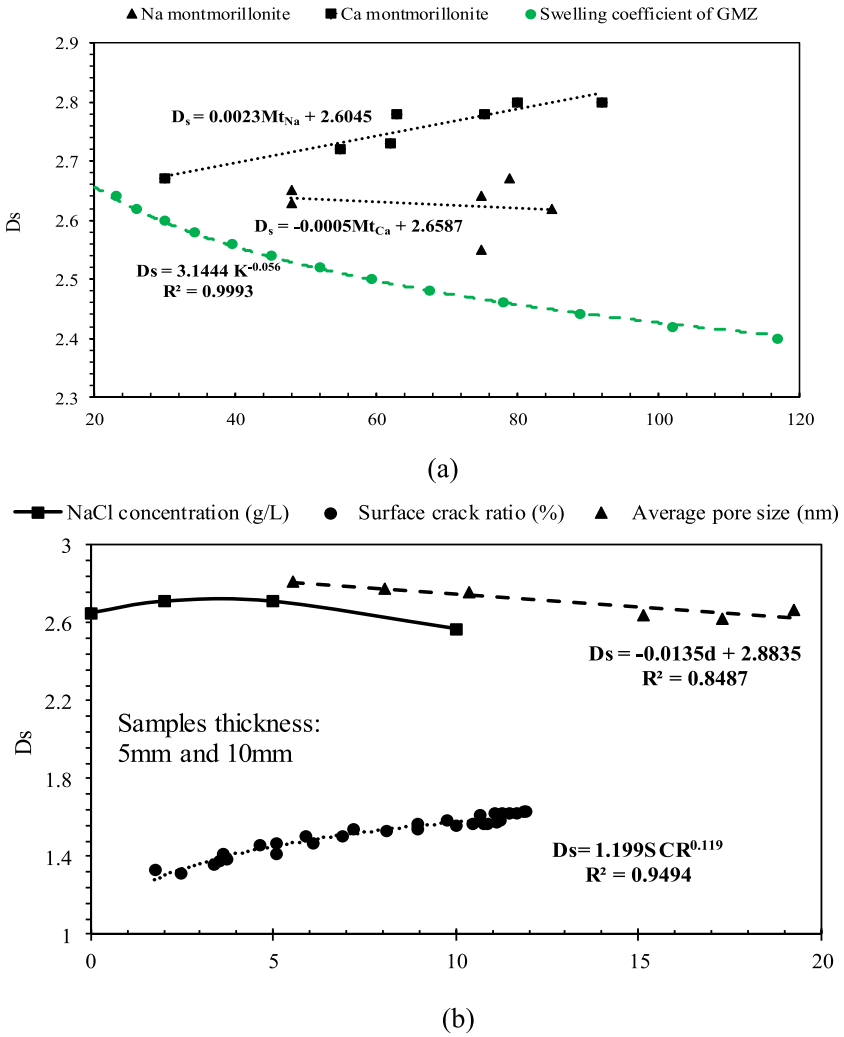

Fig. 10 (a) Variation of D_s with type of montmorillonite (Na- and Ca-) and swelling coefficient of bentonite. (b) Variation of D_s salinity, surface cracking ratio (SCR) and pore size of bentonite

variance in salt solution concentration it led to a scattered plot with regression coefficient of 61.42%. The effective cohesion lowered to 115 kPa while the internal friction angle was halved to 5.22 . The deviation of direct shear test results from Coulomb criterion in the latter case is attributed with assumption of $D_s = 2.78$ as well as the nonuniform variance between NaCl dosages ranging from 0 to 0.83 mol/L and from 0.83 mol/L to 2 mol/L.

Additionally, the volume change behavior of GMZ bentonite was discussed in viewpoint of microstructure and the mercury intrusion porosimetry (MIP) analysis; therefore, Eq. 6 was derived which determined the post-swelling void ratio of unconfined GMZ ($\rho_d = 1.7$ g/cm^3) taking into consideration the DDL effect (Mokni et al. 2014; Yu 2006).

$$e = 10^{\left[1.5-0.2cosh^{-1}(2.02p+1)\right]} \tag{6}$$

where e represents void ratio; p is pressure of repulsion of the suction or DDL; $\cosh^{-1}$ is inverse hyperbolic cosine. Moreover, the experimental data obtained from past literatures has shown that critical void ratio e_m versus p^e or e versus p^e curve of the same bentonite immersed in NaCl solution of different concentrations is expressed by a uniform line on log-log plot with a slope equaling D_s - 3 (Li et al. 2019; Li et al.).

Discussion

Classical soil mechanics is shortsighted when the P_s of expansive soils is investigated by microporosity. Expansive clayey soils in their inherent micro properties carry numerous doubts. Their combination in complex systems such as BBMs to serve as underground geological repository for disposal of HLW, and EBS to form DGR increases the uncertainties to their multipurpose functions. These simultaneous functions have impact on their functionality and the coupled effects on the material properties can be envisaged only thorough all-inclusive approaches. Where permeability is supposed to be inhibited in buffer systems, P_s undesirably varies with degree

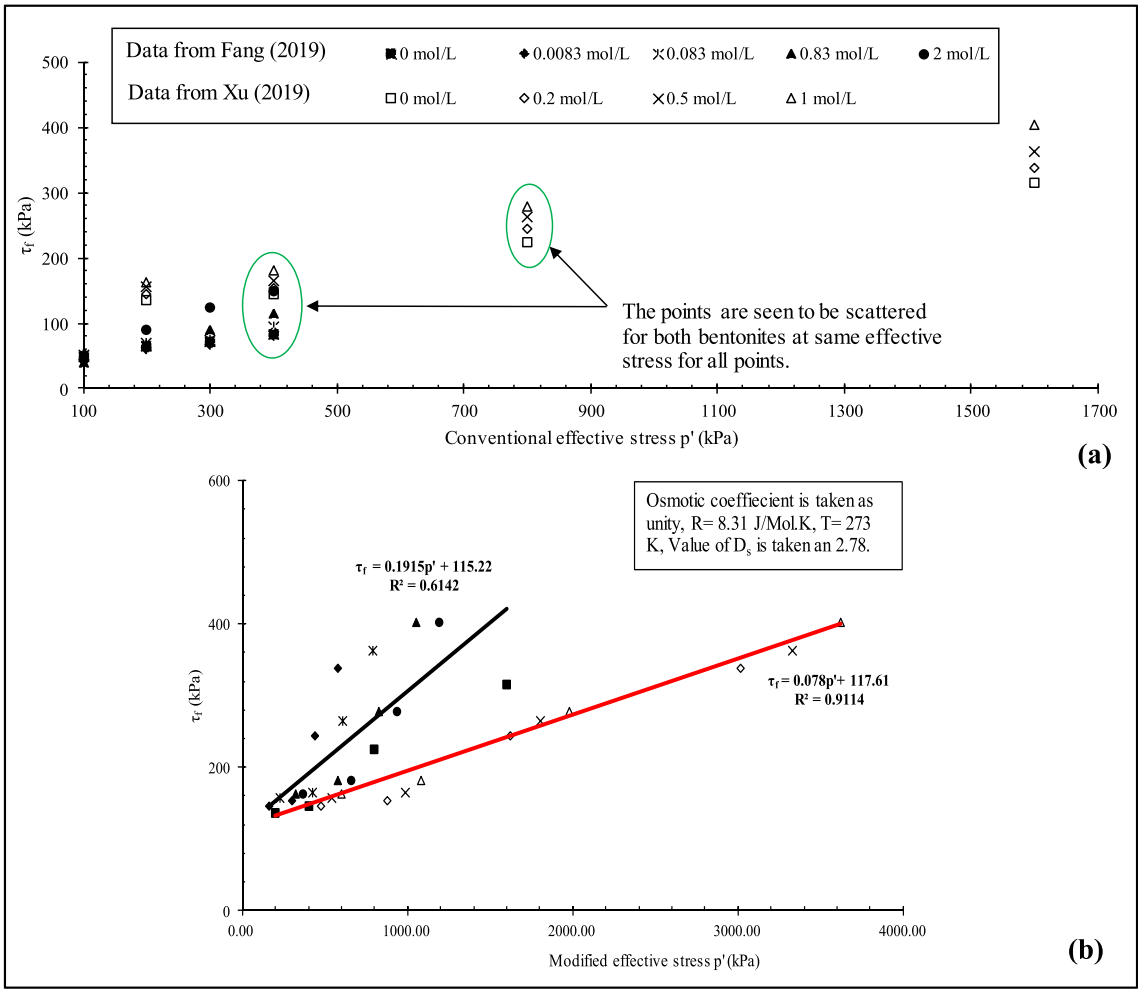

Fig. 11 Shear strength of GMZ bentonite calculated using; (a) conventional effective stress, (b) modified effective stress incorporating osmotic suction, from published data

of compaction and dry densities (Table 6). The reason could be due to different amounts of Mt within soil structure, which is most responsible for water uptake. However, it is not the absorbed water alone that contributes to the overall swelling as the buffer systems are usually delivered to contain soil soluble contaminations. So, it is justified to consider several solute concentrations when the P_s is meant to be calculated. Table 6 illustrates the important geotechnical properties of prominent bentonites that have been picked from the previous literature.

Table 6 Summary of geotechnical properties of predominant global bentonites

Bentonite	ρ_d *Mg/m³*	e -	ε_{swell} %	σ_v' *MPa*	D_s	P_s *MPa*	σ_{Yield} *MPa*	Ψ *MPa*	Wc %	References
Calcigel	1.56	0.97	-	1	2.72	1.4	-	14.3	21	(Arifin et al. 2015; Blatz et al. 2002; Cui et al. 2011; Komine 2010; Mašín and Khalili 2015; Schanz and Al-Badran 2014; Xu 2019; Ye et al. 2010a)
GMZ †	1.50	0.98	-	1	2.78	1.1	1.2	24.6	21	
FEBEX	1.50	0.8	0.09	1	2.80	3.5	4	10.9	19	
FoCa7	1.50	0.5	-	0.7	2.80	0.7	-	11.9	22	
Avonseal	1.31	1.5	-	1	2.67	2.6	3.7	14.8	19	
Kunigel	1.50	-	50	0.06	2.62	0.5	-	40.3	20	
MX-80	1.60	-	3.1	0.35	2.62	5.8	3.7	76.5	16	

Note: ρ_d dry density, e void ratio, ε_{swell} swelling strain, σ_v' effective overburden stress, σ_{Yield} yield stress

† $k = 1.1\times10^{-12}$ m/s, $\alpha = 2\times10^{-4}$ / C coefficient of thermal expansion, For: NaCl solution; cohesion = 8 kPa, internal angle of friction = 4.8

To calculate P_s of inundated bentonites with different concentrations of solutions, several methods have been proposed based on hydro mechanical characteristics. Among those, Zhang et al. (2019a) introduced a critical void ratio for highly compacted GMZ bentonite inundated with NaCl solution and incorporated both the double-layer swelling and the crystalline swelling. It was found that at a larger void ratio than the critical value, the P_s is inversely related to the concentration of NaCl solution. But, their assumptions were based on a critical void ratio regardless of the variation of effective pressures or higher rate of increase in suction while being inundated in solution with time leading to the critical state. In addition, the salt solution concentration was found to have negligible effects on P_s when the void ratio equaled the critical value. However, Cui (2017) produced smaller values using constant-volume methods as a broader concept of Zhang et al. (2019a) critical void ratio thereby indicating that the latter methods tend to report higher value of P_s when a certain critical void ratio is determined. In order to measure the anisotropy, the anisotropy coefficient C_a is a dimensionless number that is the ratio between radial SP to the axial SP. According to Cui (2017), the dry densities of bentonites are classified as; Low (> 1.1 Mg/m^3), medium (1.16 Mg/m^3 to 1.3 Mg/m^3) and high (> 1.3 Mg/m^3), for which anisotropy coefficient C_a ranges from 0.82 to 0.48 (highly anisotropic and no microstructure collapse), 0.76 to 0.9 (almost isotropic and greater microstructure collapse), and close to unity (medium anisotropic and limited microstructure collapse), respectively. Findings of both Cui (2017) and Zhang et al. (2019a) accentuate recent suggestions by Middelhoff et al. (2020) that duration of inundation also has a major role on the pore water effect specially at longer durations when salt presence decreases P_s while at shorter periods this effect is not that significant. Consequently, along with determination of a critical void ratio, solution chemistry influence on pore space should also be considered in different time periods.

Akinwunmi et al. (2019) studied the influence of temperature on the P_s at three different temperature ranges. It was revealed that at 300 Kelvin (K), an exponential decrease in P_s is observed that is associated with increase in d-spacing and reduction in dry density of compacted bentonite. P_s rises due to increased dry density such that increase in P_s at low dry density is not significant, between the range of 300 and 600 K. The P_s is recorded to exhibit highest value at 250 K within the range of 150 to 300 K (Akinwunmi et al. 2019). In addition, the P_s of densely compacted bentonite subjected to elevated temperature has been reported to lower down according to Kale and Ravi (2019) which also led to stoichiometric dissolution of magnesium and silicon at 110 °C and also changed the ratio of dissolved Mg/Si (Kaufhold et al. 2019). However, the increase in P_s is also reported with increasing temperature because the interlayer spacing is increased and the diffusion coefficient of water also increases (Akinwunmi et al. 2019). The exposure of bentonite to elevated temperature will reduce the undrained shear strength, however, for the samples subjected to temperature of 200 C prior to compaction, Dueck and Börgesson (2015) reported that the mechanical properties of clay remain unchanged.

At a variety of dry densities and temperature ranges, the saturated hydraulic conductivity (k_{sat}) of GMZ bentonite has been found to lower down at higher dry densities. The k_{unsat} is important to be calculated considering constraint conditions in order to evaluate the feasibility of densely compacted GMZ bentonite as engineered barrier in the DGR. The k_{unsat} of confined GMZ is calculated (ρ_d=1.7 g/cm^3) and it ranges from 1.13×10^{-13} m/s and 8.41×10^{-15} m/s, while it rises for higher suction values (up to 70 MPa) and is recorded to drop with further increase in suction till 80 MPa. According to Ören and Akar (2017) and Biju and Arnepalli (2020), the permeability values in the case of landfill leaches were found to range from 2.3×10^{-12} m/s and 2.0×10^{-11} m/s. On the other hand, Ye et al. (2010a) found that the k_{unsat} of unconfined GMZ was approximately 1.0×10^{-14} m/s. It appears that this value is attained gradually with the increase in suction however some variations at the beginning and final stages are experienced while conducting experiments. Note that, k_{unsat} of unconfined densely compacted GMZ is greater in the case of confined bentonite which is attributed to changes brought in microstructure when water is added for various constraint conditions. Moreover, the decrease in hydraulic conductivity with increasing dry density is higher in compacted bentonites which could be associated with higher degree of compaction. The coefficient of thermal expansion of compacted GMZ bentonite is 2×10^{-4} / C (Table 6). At saturation degrees more than 20%, the thermal conductivity and saturation show linear behavior (Cui et al. 2011; Liu et al. 2007). This clearly shows that the dry density significantly affects the two important properties including P_s and hydraulic conductivity of expansive clays and bentonite-based materials.

The presence of saline solution leads to development of osmotic suction π due to which compacted BBMs undergo reduction in swelling parameters. The engineering behavior of expansive clays is affected by the salt concentration in pore water solution and the volume change is brought as a result of salt contentration difference (referred to as “osmotic suction” in unstaurated soil mechanics) between regions formed in the soil due to osmotic or osmotically iduced consolidation (Bulolo and EC L 2019). It is believed that osmotic component of suction has the governing dominance in saline solution even for solutes with lesser salt concentration, however due to repulsive forces, which adds to the external forces, the net stress equilibrium maintains the primary effect on the shear strength and compressibility of inundated bentonites in saline solutions which contradicts the findings of Miller and Nelson (2006) thus demarcating the negligible effect of matric suction on total suction. Thyagaraj and Salini (2015) found by SEM

test results that with the increase in pore fluid osmotic suction, aggregation will occur due to decrease in the double layer that leads to reduced micropores and large macropores. The degree of saturation of these macropores drop thus increasing the matric suction as a result (Thyagaraj and Salini 2015). Because the DDL size depends on the concentration of ions in the solution, with increasing osmotic suction the DDL size reduces and thus the interparticle repulsion is also decreased (Mašín and Khalili 2015). The most conventional method of determining osmotic suction is through Van't Hoff equation, however due to neglecting many parameters in the equation, Li et al. (2019) developed Simplified Debye-Hückel (SDH) equation after Pitzer and Mayagora to determine more reliable values of osmotic suction. Increase in osmotic suction showed delay in reaching swelling strain which is also observed in osmotic consolidation as well as swelling of Na- montmorillonite (Arifin and Schanz 2009).

The surface fractal dimension (D_s) is highly related to the osmotic suction of the compacted mixture, for instance, in the calculation of peak shear strength of saline solutions. D_s is a measure of surface roughness or irregularities. SFD or D_s means the surface fractal dimension and is an efficacious parameter for characterizing the buffer/backfill properties of bentonite and it can also successfully predict other important characteristics such as swelling capacity, hydraulic conductivity, and surface absorbability (Xiang et al. 2019b). It is imperative due to its connection with real-world data. Its applications are found in various important physico-chemical processes such as adsorption. Celis et al. (1998) calculated D_s and the critical exponent (S) in FHH model from the NAIT results. In addition, D_s of rough membrane surface is yielded by analyzing the atomic force microscopy (AFM) image data by employing power spectrum method (Cai et al. 2017). Xu et al. (2014) explained the effect of osmotic suction quantitatively after determining the D_s of Tsukinuno bentonite by NAIT and proposed a modified form of the effective stress incorporating with osmotic suction. Guerin et al. (2019) revealed that the morphological fractal dimension is insufficient to replicate and explain the flocs shape in contrast to the D_s calculated by diffraction measurements which better describes the average trend of largest available aggregate size. Xiang et al. (2019b) studied the change mechanism of D_s in commercial Na-bentonite because of corrosion by alkaline solution and found that the e_m versus P_s curves were obtained for all tested cases revealed negligible effect of alkaline corrosion on D_s. Avnir and Jaroniec (1989) used the FHH equation for calculating D_s that relates the adsorbed nitrogen by the bentonite and the corresponding relative air pressure. The resemblance of molecular diameter of N_2 and hydrone render the NAIT suitable method to describe the water absorbed by FHH equation. Furthermore, D_s is also calculated by the swell deformation test undertaken in laboratory with limitation of vertical overburden pressure, i.e., P_s equaling the total suction Ψ in bentonite. The D_s obtained from swelling deformation are similar to that of FHH equation. Hence, it is a reasonable technique for determining D_s. The FHH model is based on multilayer adsorption whereas Neimark method is a model independent and the D_s from the latter is comparatively lesser due to surface being characterized by larger pores ($r > 2$nm). In addition, the Freundlich isotherm model yields smaller D_s values than the FHH isotherm model. The latter and the SAXS techniques are comparatively accurate and complex as the liquid-phase adsorption involves greater complications as compared with vapor-phase adsorption.

Finally, the shear strength of the unsaturated expansive clays is one of the major characteristics needed in geotechnical engineering designs (Zhai et al. 2019), and it has been concluded that the stress strain behavior of bentonite subjected to undrained shearing depends on temperature, stress, strain, dry density, water content, saturation, gypsum content, exchangeable cations etc. (Dueck and Börgesson 2015). Leong and Abuel-Naga (2018) performed UCS tests on compacted low plasticity silt specimens at specified intervals and found that the compression strength remain unchanged at similar moisture content and was independent of time and pore water type. Additionally, the set of specimens experiencing osmotic suction gradient did not affect the shear strength of soil which leads to the conclusion that the effect of osmotic suction on shearing strength of aforementioned soil was minimal. Among many researches available, Zhang et al. (2016) revealed that the increase of NaCl concentration significantly enhances the shear strength of GMZ bentonite at same vertical pressure whereas, Dutta and Mishra (2016) studied the effect of saline solutions such as NaCl and $CaCl_2$ of different concentrations on the volume changes of two compacted and mineralogically different bentonites. It was found that a unique line depicted the void ratios of the same bentonite in different concentrations of alkaline solutions. Moreover, the decrease of Mt content in the bentonite due to alkali corrosion from NaOH or Na_2CO_3 leads to reduction of adsorption capacity, SSA, and swelling capacity (Xiang et al. 2019b). Results of experimental study conducted by Bulolo and EC L (2019) on highly expansive clay in saline solution concluded that upon application of mechanical stress an extra settlement along with the consolidation settlement is generated due to the osmotic suction, however the soil compressibility remains unaffected. Hence, the peak shear strength of GMZ bentonite exhibits a significant variation when it is calculated using fractal approach wherein a unique line defines the strength relationship at numerous levels of saline concentrations.

Conclusion

GMZ bentonite is one of significant highly expansive clays in China. It has been studied in terms of mineralogical

characteristics and chemical composition, hydromechanical and chemical behavior, swelling nature, temperature effects, microstructure, and volume change and compression behavior. Upon extensive literature review of reviewing 217 research studies, this review article incorporates the achievements of recent trends in investigating the hydromechanical behavior and the theoretical fractal approach to bentonites-based materials BBMs over past two decades with focus on GMZ bentonite as engineered barrier/backfilling material in the Chinese program of high-level nuclear waste disposal.

1. The water retention capacity of the densely compacted Na-GMZ bentonite lowers with elevation of temperature, irrespective of confining conditions. The water retention curves (WRCs) suggest that water rests inside bentonite and it is noted that in range of low suction the WRCs are significantly affected by the confining conditions whereas ~~the~~ in the range of high suction the effect of confinement appears to have no effect on the WRCs, which is due to process of exfoliation in clay particles.
2. With the increase in dry density and moisture content, the thermal conductivity of BBMs is greater than the pure GMZ bentonite, whereas the hydraulic conductivity on saturation initially lowers and increases afterwards with reduction in suction that is also consistent with behavior of macro-pore volume observed during the mercury intrusion porosimetry tests. At the same suction, the unsaturated permeability of GMZ bentonite in unconfined case is greater than in confined state that could be because of various microstructural transformations when confined. At very low suction values, the macro-pore volume rises due to the presence of pores that leads to an increase in permeability. It is clear from the results that with temperature rising and diminishing dry density the permeability increases. At greater suctions than 20 MPa, temperature effect is more pronounced as the water uptake of bentonites at lower suctions is attributed to microstructural level where thermal effect at micro level is neglected.
3. For salt amended solutions, the osmotic suction can be effectively calculated using modified Pitzer and Mayagora equation that is further used in obtaining the modified effective stress P^e using the fractal approach in expansive clays to which the bentonite in salt solution is subjected. After that, the swelling characteristics and compression behavior of BBMs inundated in salt solutions are quantified using the fractal equation that incorporates the osmotic suction effect. Moreover, the microstructural characteristics assist in describing the mechanical behavior of clays in viewpoint of water chemical potentials related to osmotic suctions. This suggests that the use of fractal theory to explain the hydromechanical behavior of bentonites assists in simplifying the existing knowledge, which is analyzed using conventional effective stress equation.
4. Nitrogen adsorption isotherm test (NAIT) and SAXS are concluded to be accurate methods for calculating D_s along with Frenkel−Halsey−Hill (FHH) model. The D_s of bentonite can be determined by easy-to-perform swelling deformation tests. D_s obtained from swelling deformation are similar to that of the FHH equation. D_s from Neimark model are smaller than obtained by the FHH because surface is characterized by larger pores ($r >$ 2nm) where capillary condensation occurs. In addition, Freundlich method also yields lesser values than the FHH equation.
5. Subsequent swelling induced after completion of crystalline swelling is attributed to the osmotic process and is called the osmotic or double layer swelling. Osmotic suction component comes from dissolved solutes in soil porewater and bentonites. The osmotic efficiency is the extent to which the bentonite acts as a fully semipermeable membrane. Modified effective stress incorporates the effect of osmotic suction and has been found to follow fractal nature by exhibiting a unique straight line on logarithmic scale. The proposed subsequent formula is based on fractal model for the surface of clay structure such that osmotic suction is determined from the Van't Hoff equation and the volume change behavior of expansive soils can be expressed by the aforementioned curve of $e–p_e$ which is also validated by experimental data.
6. With the knowledge of available literature and to understand the recent progresses of fractal theory, the equations governing in determining the swell deformation and strength characteristics, along with correlations between swelling parameters and suction were gathered and represented in Tables 4 and 5, respectively. In addition, Table 1 gives a succinct idea about various physical, chemical and geotechnical properties of the predominant global bentonites used for the disposal of nuclear waste.

Future recommendations

As compared to the investigations on the rest of bentonites across the world, it can be seen that GMZ bentonite has been studied to a limited extent in terms of hydromechanical and swelling behavior however the progresses of fractal application in GMZ bentonite in contrast to other bentonites appears to be studied in more detail. In addition, keeping in view the complexity of coupled conditions involving thermal, hydraulic, mechanical and chemical (T-H-M-C) processes that acts simultaneously in the geological repository waste, issues such as thermal effects on the properties of the GMZ bentonite-based materials, the hydraulic behavior of the contact surface between the GMZ bentonite and the granite has been scarcely studied the sealing properties of the GMZ BBMs subjected to

T-H-M-C coupled conditions, for instance, should be researched in future. Furthermore, the effect of electrostatic forces to shear strength and compression characteristics until date are inconsistent and need further research.

List of abbreviations: FSSS, fully softened shear strength; RMSE, root mean square error; HLW, high level nuclear waste; DGR, deep geological repository; GMZ, GaoMiaoZi bentonite; EBS, engineered barrier system; SFD, surface fractal dimension; NAIT, nitrogen adsorption isotherm technique; SAXS, small-angle X-ray scattering; FHH, Frenkel−Halsey −Hill model; CEC , cation exchange capacity; SSA, specific surface area; LOI, loss on ignition; XRF, x-ray fluorescence analysis; XRD, x-ray diffraction analysis; SEM, scanning electron microscopy; TEM, transmission electron microscopy; MIP, mercury intrusion porosimetry; DDL, diffuse double layer; WRC, water retention curve; UCS, unconfined compressive strength; AFM, atomic force microscopy; ANN, artificial neural network; MAE, mean absolute error; NSE, Nash-Sutcliffe efficiency; LL, liquid limit; PL, plastic limit; PI, plasticity index; E-F, edge to face orientation; F-F, face to face orientation; Mt, montmorillonite**List of symbols** π or h_π, osmotic suction; Ψ or h_t, total suction; h_m, matric suction; D_s, surface fractal dimension; σ^S, structural stress; σ^M, mineral stress; $\sigma^{R\text{-}A}$, interparticle stress; e_m, void ratio of swelled Mt; P_s, swell pressure; p_s, vertical stress; ω, water content (%); ρ_d, dry density (Mg/m^3); G_s, specific gravity; k_{sat}, saturated hydraulic conductivity; k_{unsat}, unsaturated hydraulic conductivity; C_a, anisotropy coefficient; e_c, critical void ratio; P^e or P', modified effective stress (with h_π); P_i, performance index

Author contribution FJ: Writing—original draft preparation, methodology, investigation, data curation; YX: conceptualization, supervision; XL: writing—reviewing and editing; BJ: visualization, writing—reviewing and editing; MI: reviewing

Funding The Key project of the National Natural Science Foundation of China (Grant no. 41630633), National Key Research and Development Project (Grant No. 2019YFC1509800), and Key Special Project of the Ministry of Science and Technology of the People's Republic of China for Monitoring, Warning and Prevention of Major Natural Disasters.

Data availability All data generated or analyzed during this study are included in this published article.

Declarations

Ethics approval Not applicable

Consent to participate Not applicable

Consent for publication The manuscript is original and unpublished and is not being considered for publication elsewhere. The authors allow this review paper to be published upon acceptance in the Journal of Environmental science and pollution research.

Competing interests The authors declare no competing interests.

References

Abdou M, Al-Sabagh A, Dardir M (2013) Evaluation of Egyptian bentonite and nano-bentonite as drilling mud Egyptian. J Pet 22:53–59

Abdullahi S, Audu A (2017) Comparative analysis on chemical composition of bentonite clays obtained from Ashaka and tango deposits in Gombe State. Nigeria ChemSearch Journal 8:35–40

Afzal S, Shahzada K, Fahad M, Saeed S, Ashraf M (2014) Assessment of early-age autogenous shrinkage strains in concrete using bentonite clay as internal curing technique. Constr Build Mater 66:403–409

Agarwal S (2006) Pozzolanic activity of various siliceous materials. Cem Concr Res 36:1735–1739

Agus SS, Schanz T (2008) A method for predicting swelling pressure of compacted bentonites. Acta Geotech 3:125

Akinwunmi B, Sun L, Hirvi JT, Kasa S, Pakkanen TA (2019) Influence of temperature on the swelling pressure of bentonite clay. Chem Phys 516:177–181

Al-Jariri JS, Khalili F (2010) Adsorption of Zn (II), Pb (II), Cr (III) and Mn (II) from water by Jordanian bentonite. Desalin Water Treat 21:308–322

Alves J, Zanini A, De Souza M, Nascimento M (2016) Study of selection and purification of Brazilian bentonite clay by elutriation: a XRF. SEM and Rietveld analysis Cerâmica 62:1–8

Angar Y, Djelali N-E, Kebbouche-Gana S (2017) Investigation of ammonium adsorption on Algerian natural bentonite. Environ Sci Pollut Res 24:11078–11089

Arifin YF, Schanz T (2009) Osmotic suction of highly plastic clays. Acta Geotech 4:177–191

Arifin YF, Utami UBL, Schanz T (2015) Physico-Hydro-Mechanical Properties of a Commercial Bentonite in Indonesia. In: Proc the 14th Int Conf on Quality in Research (QIR)

Avnir D, Jaroniec M (1989) An isotherm equation for adsorption on fractal surfaces of heterogeneous porous materials. Langmuir 5:1431–1433

Baltrėnaitė E, Lietuvninkas A, Baltrėnas P (2018) Biogeochemical and engineered barriers for preventing spread of contaminants. Environ Sci Pollut Res 25:5254–5268

Barakan S, Aghazadeh V (2020) The advantages of clay mineral modification methods for enhancing adsorption efficiency in wastewater treatment: a review. Environ Sci Pollut Res:1–28

Barbour S, Fredlund D (1989) Mechanisms of osmotic flow and volume change in clay soils. Can Geotech J 26:551–562

Biju M, Arnepalli D (2020) Effect of biopolymers on permeability of sand-bentonite mixtures. J Rock Mech Geotech Eng 12:1093–1102

Blatz J, Graham J, Chandler N (2002) Influence of suction on the strength and stiffness of compacted sand bentonite. Can Geotech J 39:1005–1015

Briggs S, McKelvie J, Sleep B, Krol M (2017) Multi-dimensional transport modelling of corrosive agents through a bentonite buffer in a Canadian deep geological repository. Sci Total Environ 599:348–354

Bulolo S, EC L (2019) Osmotic consolidation of expansive soil Japanese Geotechnical Society Special. Publication 7:256–260

Bulut R, Lytton RL, Wray WK (2001) Soil suction measurements by filter paper. Expansive clay soils and vegetative influence on shallow foundations, In, pp 243–261

Cai X et al (2017) Influences of fractal dimension of membrane surface on interfacial interactions related to membrane fouling in a membrane bioreactor. J Colloid Interface Sci 500:79–87

Calvello M, Lasco M, Vassallo R, Di Maio C (2005) Compressibility and residual shear strength of smectitic clays: influence of pore aqueous solutions and organic solvents. Italian Geotechnical Journal 1:34–46

Cara S, Carcangiu G, Padalino G, Palomba M, Tamanini M (2000) The bentonites in pelotherapy: thermal properties of clay pastes from Sardinia (Italy). Appl Clay Sci 16:125–132

Castellanos E, Villar M, Romero E, Lloret A, Gens A (2008) Chemical impact on the hydro-mechanical behaviour of high-density FEBEX bentonite Physics and Chemistry of the Earth. Parts A/B/C 33:S516–S526

Castillo O, Melin P (2020) Forecasting of COVID-19 time series for countries in the world based on a hybrid approach combining the fractal dimension and fuzzy logic Chaos. Solitons & Fractals 140: 110242

Celis R, Cornejo J, Hermosin M (1998) Textural properties of synthetic clay-ferrihydrite associations. Clay Miner 33:395–407

Chen L, Wang J, Liu Y, Collin F, Xie J (2012) Numerical thermo-hydro-mechanical modeling of compacted bentonite in China-mock-up test for deep geological disposal. J Rock Mech Geotech Eng 4:183–192

Chen X, Li T, Shen J, Hu Z (2016) Fractal design of microfluidics and nanofluidics—a review. Chemom Intell Lab Syst 155:19–25

Chen Y-G, Dong X-X, Zhang X-D, Ye W-M, Cui Y-J (2018) Combined thermal and saline effects on the swelling pressure of densely compacted GMZ bentonite. Appl Clay Sci 166:318–326

Christopher IC, Chimobi ND (2019) Emerging trends in expansive soil stabilisation. A review Journal of Rock Mechanics and Geotechnical Engineering

Churchman GJ, Askary M, Peter P, Wright M, Raven MD, Self PG (2002) Geotechnical properties indicating environmental uses for an unusual Australian bentonite. Appl Clay Sci 20:199–209

Cui Y-J (2017) On the hydro-mechanical behaviour of MX80 bentonite-based materials. J Rock Mech Geotech Eng 9:565–574

Cui Y-J, Tang AM (2013) On the chemo-thermo-hydro-mechanical behaviour of geological and engineered barriers. J Rock Mech Geotech Eng 5:169–178

Cui Y-J, Tang AM, Loiseau C, Delage P (2008) Determining the unsaturated hydraulic conductivity of a compacted sand–bentonite mixture under constant-volume and free-swell conditions. Physics and Chemistry of the Earth, Parts A/B/C 33:S462–S471

Cui Y-J, Tang A-M, Qian L-X, Ye W-M, Chen B (2011) Thermal-mechanical behavior of compacted GMZ. Bentonite Soils and foundations 51:1065–1074

Das SK (2013) 10 Artificial Neural Networks in Geotechnical Engineering. Modeling and Application Issues Metaheuristics in Water Geotech Transp Eng 45:231–267

Di Maio C (1996) The influence of pore fluid composition on the residual shear strength of some natural clayey soils. In: VII international symposium on landslides:1189–1194

DI MAIOĆ C (1996) Exposure of bentonite to salt solution: osmotic and mechanical effects. Geotechnique 46(4):695–707

Di Maio C, Santoli L, Schiavone P (2004) Volume change behaviour of clays: the influence of mineral composition, pore fluid composition and stress state. Mech Mater 36:435–451

Dixon DA (2000) Porewater salinity and the development of swelling pressure in bentonite-based buffer and backfill materials. Posiva Oy

Dueck A, Börgesson L (2015) Thermo-mechanically induced brittleness in compacted bentonite investigated by unconfined compression tests. Eng Geol 193:305–309

Dutta J, Mishra AK (2016) Consolidation behaviour of bentonites in the presence of salt solutions. Appl Clay Sci 120:61–69

Er-ramly A, Ider A (2014) Physico-chemical and mineralogical characterization of a Moroccan bentonite (Azzouzet) and determination of its nature and its chemical structure. International Journal of Materials Science and Applications 3:42

Faghihian H, Godazandeha N (2009) Synthesis of nano crystalline zeolite Y from bentonite. J Porous Mater 16:331–335

Fang Y-g, Ou Z-f, Li B (2019) Effect of Pore Fluid Concentration on Shear Strength of Soft Clay Soil. Mechanics and Foundation Engineering 56:265–272

Fanti F (2009) Bentonite chemical features as proxy of late Cretaceous provenance changes: A case study from the Western Interior Basin of Canada. Sediment Geol 217:112–127

Fattah MY, Al-Lami AH (2016) Behavior and characteristics of compacted expansive unsaturated bentonite-sand mixture. J Rock Mech Geotech Eng 8:629–639

Fernández-Martínez M, Guirao JLG, Sánchez-Granero MÁ, Segovia JET (2019) Hausdorff Dimension Type Models for Fractal Structures. Fractal Dimension for Fractal Structures. Springer, In, pp 149–195

Fredlund DG, Xing A (1994) Equations for the soil-water characteristic curve. Can Geotech J 31:521–532

Fukushi K, Sugiura T, Morishita T, Takahashi Y, Hasebe N, Ito H (2010) Iron–bentonite interactions in the Kawasaki bentonite deposit. Zao area, Japan Applied geochemistry 25:1120–1132

Gandomi AH, Roke DA (2015) Assessment of artificial neural network and genetic programming as predictive tools. Adv Eng Softw 88: 63–72

Gareche M, Allal A, Zeraibi N, Roby F, Azril N, Saoudi L (2016) Relationship between the fractal structure with the shear complex modulus of montmorillonite suspensions. Appl Clay Sci 123:11–17

Gates W, Anderson JS, Raven MD, Churchman G (2002) Mineralogy of a bentonite from Miles Queensland, Australia and characterisation of its acid activation products. Appl Clay Sci 20:189–197

Gens A (2019) Clays in natural and engineered barriers for nuclear waste disposal. Elsevier

Gimenez D, Perfect E, Rawls W, Pachepsky Y (1997) Fractal models for predicting soil hydraulic properties: a review. Eng Geol 48:161–183

Gouze P, Noiriel C, Bruderer C, Loggia D, Leprovost R (2003) X-ray tomography characterization of fracture surfaces during dissolution. Geophys Res Lett:30

Gueddouda M, Goual I, Benabed B, Taibi S, Aboubekr N (2016) Hydraulic properties of dune sand–bentonite mixtures of insulation barriers for hazardous waste facilities. J Rock Mech Geotech Eng 8: 541–550

Guerin L, Frances C, Liné A, Coufort-Saudejaud C (2019) Fractal dimensions and morphological characteristics of aggregates formed in different physico-chemical and mechanical flocculation environments. Colloids Surf A Physicochem Eng Asp 560:213–222

Guo H, He M, Sun C, Li B, Zhang F (2012) Hydrophilic and strength-softening characteristics of calcareous shale in deep mines. J Rock Mech Geotech Eng 4:344–351

He Y (2016) Real-world solutions for improving estimates of land-atmosphere exchanges in heterogeneous landscapes. Prifysgol Bangor University

He Y, Chen Y-G, Ye W-M, Chen B, Cui Y-J (2016) Influence of salt concentration on volume shrinkage and water retention characteristics of compacted GMZ bentonite. Environ Earth Sci 75:535

He Y, Ye W-M, Chen Y-G, Cui Y-J (2019a) Effects of K+ solutions on swelling behavior of compacted GMZ bentonite. Eng Geol 249: 241–248

He Y, K-n Z, Wu D-y (2019b) Experimental and modeling study of soil water retention curves of compacted bentonite considering salt solution effects. Geofluids:2019

Herbert E, Oliver W, Pharr G (2008) Nanoindentation and the dynamic characterization of viscoelastic solids. J Phys D Appl Phys 41: 074021

Horpibulsuk S, Yangsukkaseam N, Chinkulkijniwat A, Du YJ (2011) Compressibility and permeability of Bangkok clay compared with kaolinite and bentonite. Appl Clay Sci 52:150–159

Huff W, Merriman R, Morgan D, Roberts B (1993) Distribution and tectonic setting of Ordovician K-bentonites in the United Kingdom. Geol Mag 130:93–100

Iqbal MF, Liu Q-F, Azim I, Zhu X, Yang J, Javed MF, Rauf M (2020) Prediction of mechanical properties of green concrete incorporating waste foundry sand based on gene expression programming. J Hazard Mater 384:121322

Jalal F-E, Xu Y, Jamhiri B, Memon SA (2020) On the Recent Trends in Expansive Soil Stabilization Using Calcium-Based Stabilizer Materials (CSMs). A Comprehensive Review Advances in Materials Science and Engineering 2020(1510969):1–23. https://doi.org/10.1155/2020/1510969

Jalal FE, Xu Y, Iqbal M, Javed MF, Jamhiri B (2021) Predictive modeling of swell-strength of expansive soils using artificial intelligence approaches: ANN. ANFIS and GEP Journal of Environmental Management 289:112420

Jaroniec M (1995) Evaluation of the fractal dimension from a single adsorption isotherm. Langmuir 11:2316–2317

Jia L-Y, Chen Y-G, Ye W-M, Cui Y-J (2019) Effects of a simulated gap on anisotropic swelling pressure of compacted GMZ bentonite. Eng Geol 248:155–163

Jiang H, Xiang G, Xu Y, Chen T (2014) Study on the Swelling Mechanism and Characteristics of Bentonite. Soil Behavior and Geomechanics, In, pp 43–53

Kale RC, Ravi K (2019) Influence of thermal history on swell pressures of compacted bentonite. Process Saf Environ Prot 123:199–205

Kaufhold S, Baille W, Schanz T, Dohrmann R (2015) About differences of swelling pressure—dry density relations of compacted bentonites. Appl Clay Sci 107:52–61

Kaufhold S, Dohrmann R, Degtjarev A, Koeniger P, Post V (2019) Mg and silica release in short-term dissolution tests in bentonites. Appl Clay Sci 172:106–114

Kiipli T, Radzevičius S, Kallaste T, Motuza V, Jeppsson L, Wickström LM (2008) Wenlock bentonites in Lithuania and correlation with bentonites from sections in Estonia. Sweden and Norway GFF 130: 203–210

Kim Y-S, Tran TQ, G-o K, Do TM (2019) Stabilization of a residual granitic soil using various new green binders. Constr Build Mater 223:724–735

Komine H (2004a) Simplified evaluation for swelling characteristics of bentonites. Eng Geol 71:265–279

Komine H (2004b) Simplified evaluation on hydraulic conductivities of sand–bentonite mixture backfill. Appl Clay Sci 26:13–19

Komine H (2010) Predicting hydraulic conductivity of sand–bentonite mixture backfill before and after swelling deformation for underground disposal of radioactive wastes. Eng Geol 114:123–134

Komlósi A, Kuzmann E, Nagy NM, Homonnay Z, Kubuki S, Kónya J (2007) Incorporation of Fe in the interlayer of Na-bentonite via treatment with FeCl3 in acetone. Clay Clay Miner 55:89–95

Kravchenko A, Zhang R (1998) Estimating the soil water retention from particle-size distributions: a fractal approach. Soil Sci 163:171–179

Lang A (1967) Osmotic coefficients and water potentials of sodium chloride solutions from 0 to 40 C. Aust J Chem 20:2017–2023

Lathrop JI, Lutz JH, Summers SM (2009) Strict self-assembly of discrete Sierpinski triangles. Theor Comput Sci 410:384–405

Lee J-O, Park J-H, Cho W-J (2006) Engineering-scale Validation Test for the THM Behaviors of a HLW Disposal System. Journal of Nuclear Fuel Cycle and Waste Technology (JNFCWT) 4:197–207

Lee JO, Lim JG, Kang IM, Kwon S (2012) Swelling pressures of compacted Ca-bentonite. Eng Geol 129:20–26

Leong E-C, Abuel-Naga H (2018) Contribution of osmotic suction to shear strength of unsaturated high plasticity silty soil. Geomechanics for Energy and the Environment 15:65–73

Li X-Y, Xu Y-f (2020) Determination and application of osmotic suction of saline solution in clay. Environ Earth Sci 79:1–14

Li X, Li C, Xu Y (2019) Representation of volume change for bentonite in saline solution based on modified effective stress KSCE. J Civ Eng 23:2065–2073

Li X, Xu Y, Li C (n.d.) Experimental study on the 1-D free swelling of compacted bentonite. Acta Geotech:1–13

Liu Y (2010) Influence of heating and water-exposure on the liquid limits of GMZ01 and MX80 bentonites Journal of Rock Mechanics and. Geotech Eng 2:188–192

Liu L (2013) Prediction of swelling pressures of different types of bentonite in dilute solutions. Colloids Surf A Physicochem Eng Asp 434:303–318

Liu X, Nie B (2016) Fractal characteristics of coal samples utilizing image analysis and gas adsorption. Fuel 182:314–322

Liu Y, Xu G, Liu S, Chen Z (2001) Study on the basic property of Gaomiaozi bentonite. Inner Mongolia, China Nuclear Information Centre

Liu Y, Cai M, Wang J (2007) Thermal conductivity of buffer material for high-level waste diaposal Chinese. Journal of Rock Mechanics and Engineering 26:3891–3896

Liu X, Zhang G, Heathman GC, Wang Y, C-h H (2009) Fractal features of soil particle-size distribution as affected by plant communities in the forested region of Mountain Yimeng. China Geoderma 154: 123–130

Liu Y et al (2014) Design and validation of the THMC China-Mock-Up test on buffer material for HLW disposal. J Rock Mech Geotech Eng 6:119–125

Liu L-N, Chen Y-G, Ye W-M, Cui Y-J, Wu D-B (2018) Effects of hyperalkaline solutions on the swelling pressure of compacted Gaomiaozi (GMZ) bentonite from the viewpoint of Na+ cations and OH–anions. Appl Clay Sci 161:334–342

Liu J, Song S, Cao X, Meng Q, Pu H, Wang Y, Liu J (2020) Determination of full-scale pore size distribution of Gaomiaozi bentonite and its permeability prediction. J Rock Mech Geotech Eng

Long Z, De-an S, Yue-miao L (2016) Comparison between swelling properties of two Gaomiaozi Na-bentonites. Rock Soil Mech 37: 3447–3454

Low PF (1980) The Swelling of Clay: II. Montmorillonites 1. Soil Sci Soc Am J 44:667–676

Lü Q, Qiu Q, Zheng J, Wang J, Zeng Q (2019) Fractal dimension of concrete incorporating silica fume and its correlations to pore structure, strength and permeability. Constr Build Mater 228:116986

Lv Q et al (2020) In situ SAXS study of fractal structure of non-caking coal during carbonisation. Philos Mag Lett:1–8

Mahamud MM, García V (2018) Textural characterization of chars using fractal analysis of N2 and CO2 adsorption. Fuel Process Technol 169:269–279

Mahto V, Sharma V (2008) Characterization of Indian bentonite clay samples for water-based drilling fluids. Pet Sci Technol 26:1859–1868

Malekani K, Rice JA, Lin J-S (1996) Comparison of techniques for determining the fractal dimensions of clay minerals. Clay Clay Miner 44:677–685

Mandelbrot BB (1983) The fractal geometry of nature vol 173, WH freeman New York

Mandelbrot B (2013) Fractals and chaos: the Mandelbrot set and beyond. Springer Science & Business Media

Martin P, Barcala J, Huertas F (2006) Large-scale and long-term coupled thermo-hydro-mechanic experiments with bentonite: the FEBEX mock-up test. J Iber Geol 32:259–282

Mašín D, Khalili N (2015) Swelling phenomena and effective stress in compacted expansive clays. Can Geotech J 53:134–147

Masindi V, Gitari MW, Tutu H, De Beer M (2015) Efficiency of ball milled South African bentonite clay for remediation of acid mine drainage. Journal of Water Process Engineering 8:227–240

Matusewicz M, Liljestroem V, Muurinen A, Serimaa R (2013) SAXS and TEM investigation of bentonite structure.

Mendhe VA, Bannerjee M, Varma AK, Kamble AD, Mishra S, Singh BD (2017) Fractal and pore dispositions of coal seams with significance to coalbed methane plays of East Bokaro. Jharkhand, India Journal of Natural Gas Science and Engineering 38:412–433

Meng D-L, D-a S, Liu Y-M (2012) Soil-water characteristic curves of Gaomiaozi bentonite-sand mixtures. Rock Soil Mech 33:509–514

Miazzo R et al (2005) Efficacy of sodium bentonite as a detoxifier of broiler feed contaminated with aflatoxin and fumonisin. Poult Sci 84:1–8

Middelhoff M, Cuisinier O, Masrouri F, Talandier J, Conil N (2020) Combined impact of selected material properties and environmental conditions on the swelling pressure of compacted claystone/bentonite mixtures. Appl Clay Sci 184:105389

Miller DJ, Nelson JD (2006) Osmotic suction in unsaturated soil mechanics. Unsaturated Soils 2006:1382–1393

Mitchell JK, Soga K (2005) Fundamentals of soil behavior. Fundamentals of soil behavior

Mohammed S (2017) Processing, effect and reactivity assessment of artificial pozzolans obtained from clays and clay wastes. A review Construction and Building Materials 140:10–19

Mokni N, Romero E, Olivella S (2014) Chemo-hydro-mechanical behaviour of compacted Boom Clay: joint effects of osmotic and matric suctions. Géotechnique 64:681–693

Mutaz E, Dafalla M (2014) Chemical analysis and X-ray diffraction assessment of stabilized expansive soils. Bull Eng Geol Environ 73: 1063–1072

Nowamooz H, Masrouri F (2010) Suction variations and soil fabric of swelling compacted soils. J Rock Mech Geotech Eng 2:129–134

Ören AH, Akar RÇ (2017) Swelling and hydraulic conductivity of bentonites permeated with landfill leachates. Appl Clay Sci 142:81–89

Pathak P (2017) An assessment of strontium sorption onto bentonite buffer material in waste repository. Environ Sci Pollut Res 24: 8825–8836

Peng L, Chen B, Pan Y (2020) Evaluation and comparison of bentonite surface fractal dimension and prediction of swelling deformation: Synchrotron radiation SAXS and N2-adsorption isotherms method. Constr Build Mater:121331

Perfect E, Kay B (1995) Applications of fractals in soil and tillage research: a review. Soil Tillage Res 36:1–20

Perrier E, Bird N, Rieu M (1999) Generalizing the fractal model of soil structure: The pore–solid fractal approach. Geoderma 88:137–164

Pfeifer P, Cole M (1990) Fractals in surface science: scattering and thermodynamics of adsorbed films. II New journal of chemistry 14(1987):221–232

Pusch R (1999) Clay colloid formation and release from MX80 buffer SKB Technical Report. TR-99-31, SKB Sweden

Pusch R (2015) Bentonite clay: environmental properties and applications. CRC Press

Raheem AM, Vipulanandan C, Joshaghani MS (2017) Non-destructive experimental testing and modeling of electrical impedance behavior of untreated and treated ultra-soft clayey soils. J Rock Mech Geotech Eng 9:543–550

Rao SM, Shivananda P (2005) Role of osmotic suction in swelling of salt-amended clays. Can Geotech J 42:307–315

Rao SM, Thyagaraj T (2007) Swell–compression behaviour of compacted clays under chemical gradients. Can Geotech J 44:520–532

Rao SM, Thyagaraj T, Rao PR (2013) Crystalline and osmotic swelling of an expansive clay inundated with sodium chloride solutions. Geotech Geol Eng 31:1399–1404

Ray S, Mishra AK, Kalamdhad AS (2021) Influence of real and synthetic municipal solid waste leachates on consolidation and shear strength behaviour of bentonites. Environ Sci Pollut Res:1–11

Reijonen HM, Kuva J, Heikkilä P (2020) Benefits of applying X-ray computed tomography in bentonite based material research focussed on geological disposal of radioactive waste. Environ Sci Pollut Res 27:38407–38421

Ren L-Q, Tong J, Li J-Q, Chen B-C (2001) Soil adhesion and biomimetics of soil-engaging components: a review. J Agric Eng Res 79:239–264

Risović D, Poljaček SM, Furić K, Gojo M (2008) Inferring fractal dimension of rough/porous surfaces—A comparison of SEM image analysis and electrochemical impedance spectroscopy methods. Appl Surf Sci 255:3063–3070

Sakizci M, Alver BE, Alver Ö, Yörükoğullari E (2010) Spectroscopic and thermal studies of bentonites from Ünye. Turkey Journal of Molecular Structure 969:187–191

Sánchez M, Gens A, Guimarães L (2012) Thermal–hydraulic–mechanical (THM) behaviour of a large-scale in situ heating experiment during cooling and dismantling. Can Geotech J 49:1169–1195

Sathyapriya S, Arumairaj P, Ranjini D (2017) Prediction of unconfined compressive strength of a stabilised expansive clay soil using ANN and regression analysis (SPSS). Asian Journal of Research in Social Sciences and Humanities 7:109–123

Schanz T, Al-Badran Y (2014) Swelling pressure characteristics of compacted Chinese Gaomiaozi bentonite GMZ01. Soils Found 54: 748–759

Shah MI, Javed MF, Abunama T (2020) Proposed formulation of surface water quality and modelling using gene expression, machine learning, and regression techniques. Environ Sci Pollut Res:1–19

Shahin MA (2013) Artificial intelligence in geotechnical engineering: applications, modeling aspects, and future directions Metaheuristics in water. geotechnical and transport engineering: 169204

Shahin MA, Jaksa MB, Maier HR (2009) Recent advances and future challenges for artificial neural systems in geotechnical engineering applications. Advances in Artificial Neural Systems:2009

Siddiqua S, Blatz J, Siemens G (2011) Evaluation of the impact of pore fluid chemistry on the hydromechanical behaviour of clay-based sealing materials. Can Geotech J 48:199–213

Sinnathamby G, Korkiala-Tanttu L, Salvador LT (2015) Shear resistance of bentonite backfill materials and their interfaces under varying hydraulic conditions in a deep rock nuclear waste repository. Appl Clay Sci 104:211–220

Sridharan A, Venkatappa Rao G (1979) Shear strength behaviour of saturated clays and the role of the effective stress concept. Geotechnique 29:177–193

Stewart D, Studds P, Cousens T (2003) The factors controlling the engineering properties of bentonite-enhanced sand. Appl Clay Sci 23: 97–110

Sun W, Fang L (2014) Swelling characteristics of Gaomiaozi bentonite and its prediction. J Rock Mech Geotech Eng 6:113–118

Sun W, Da S, Fang L, Liu S (2014) Soil-water characteristics of Gaomiaozi bentonite by vapour equilibrium technique. J Rock Mech Geotech Eng 6:48–54

Sun H, Mašín D, Boháč J (2017) Experimental characterization of retention properties and microstructure of the Czech bentonite B75. In: Proceedings of the 19th International Conference on Soil Mechanics and Geotechnical Engineering. Seoul:1249–1252

Sun Z, Y-g C, Y-j C, Xu H-d, Ye W-m WD-B (2018) Effect of synthetic water and cement solutions on the swelling pressure of compacted Gaomiaozi (GMZ) bentonite: the Beishan site case. Gansu, China Engineering Geology 244:66–74

Sun H, Mašín D, Najser J, Neděla V, Navrátilová E (2019) Bentonite microstructure and saturation evolution in wetting–drying cycles evaluated using ESEM. MIP and WRC measurements Géotechnique 69:713–726

Sun Z, Chen Y-G, Shang Y, Cui Y-J, Ye W-M, Wu D-B (2020) The sorption performance of corroded Gaomiaozi bentonite by evolved cement water at different temperatures: the case of europium removal. Environ Sci Pollut Res 27:25057–25068

Tang A-M, Cui Y-J, Le T-T (2008) A study on the thermal conductivity of compacted bentonites. Appl Clay Sci 41:181–189

Tao G, Zhu X, Cai J, Xiao H, Chen Q, Chen Y (2019) A fractal approach for predicting unsaturated hydraulic conductivity of deformable clay. Geofluids:2019

Thuc C-NH, Grillet A-C, Reinert L, Ohashi F, Thuc HH, Duclaux L (2010) Separation and purification of montmorillonite and polyethylene oxide modified montmorillonite from Vietnamese bentonites. Appl Clay Sci 49:229–238

Thyagaraj T, Salini U (2015) Effect of pore fluid osmotic suction on matric and total suctions of compacted clay. Géotechnique 65: 952–960

Tripathy S, Thomas HR, Bag R (2015) Geoenvironmental application of bentonites in underground disposal of nuclear waste: characterization and laboratory tests. Journal of Hazardous Toxic, and Radioactive Waste 21:D4015002

Tripathy A, Kumar A, Srinivasan V, Singh K, Singh T (2019) Fractal analysis and spatial disposition of porosity in major indian gas shales using low-pressure nitrogen adsorption and advanced image segmentation. Journal of Natural Gas Science and Engineering 72: 103009

Tyler SW, Wheatcraft SW (1992) Fractal scaling of soil particle-size distributions: Analysis and limitations. Soil Sci Soc Am J 56:362–369

Uddin F (2008) Clays, nanoclays, and montmorillonite minerals. Metall Mater Trans A 39:2804–2814

Villar MV, Lloret A (2004) Influence of temperature on the hydro-mechanical behaviour of a compacted bentonite. Appl Clay Sci 26:337–350

Villar MV, Lloret A (2008) Influence of dry density and water content on the swelling of a compacted bentonite. Appl Clay Sci 39:38–49

Villar MV, Gómez-Espina R, Lloret A (2010) Experimental investigation into temperature effect on hydro-mechanical behaviours of bentonite. J Rock Mech Geotech Eng 2:71–78

Wang J (2010) High-level radioactive waste disposal in China: update 2010 Journal of Rock Mechanics and. Geotech Eng 2:1–11

Wang G, Shen J, Liu S, Jiang C, Qin X (2019) Three-dimensional modeling and analysis of macro-pore structure of coal using combined X-ray CT imaging and fractal theory. Int J Rock Mech Min Sci 123: 104082

Watt-Smith MJ, Edler KJ, Rigby SP (2005) An experimental study of gas adsorption on fractal surfaces. Langmuir 21:2281–2292

Wen Z, Jintoku T (2005) Preliminary study on static mechanical property of GMZ Na-bentonite. World Nuclear Geoscience 22:211–214

Wieczorek K, Gaus I, Mayor JC, Schuster K, García-Siñeriz J-L, Sakaki T (2017) In-situ experiments on bentonite-based buffer and sealing materials at the Mont Terri rock laboratory (Switzerland) Swiss. J Geosci 110:253–268

Xi Y, Chen J, Xu Y, Chu F, Liu C (2015) Yield stress of fractal aggregates. Fractals 23:1550028

Xiang G, Jiang H, Xu Y (2014a) Surface fractal dimension of bentonite from nitrogen adsorption. Soil Behavior and Geomechanics, In, pp 286–292

Xiang G, Xu Y, Jiang H (2014b) Surface fractal dimension of bentonite and its application in calculation of swelling deformation. Surf Rev Lett 21:1450074

Xiang G, Xu Y, Jiang H (2015) Effect of Na+ on surface fractal dimension of compacted bentonite. Russ J Phys Chem A 89:870–875

Xiang G, Xu Y, Xie S, Fang Y (2017) A simple method for testing the fractal dimension of compacted bentonite immersed in salt solution. Surf Rev Lett 24:1750040

Xiang G, Xu Y, Yu F, Fang Y, Wang Y (2019a) Prediction of swelling characteristics of compacted GMZ bentonite in salt solution incorporating ion-exchange reactions. Clay Clay Miner 67:163–172

Xiang G, Ye W, Yu F, Wang Y, Fang Y (2019b) Surface fractal dimension of bentonite affected by long-term corrosion in alkaline solution. Appl Clay Sci 175:94–101

Xiangling L, Frederic B, Johan B (2006) The Belgian HLW repository design and associated R&D on the THM behavior of the host rock and EBS. Chin J Rock Mech Eng 25:681–692

Xu Y (2003) Surface fractal dimension of swelling clay minerals. Fractals 11:353–362

Xu Y (2004) Fractal approach to unsaturated shear strength. J Geotech Geoenviron 130:264–273

Xu Y (2018) Fractal model for the correlation relating total suction to water content of bentonites. Fractals 26:1850028

Xu Y (2019) Peak shear strength of compacted GMZ bentonites in saline solution. Eng Geol 251:93–99

Xu Y, Dong P (2004) Fractal approach to hydraulic properties in unsaturated porous media Chaos. Solitons & Fractals 19:327–337

Xu J, Lacidogna GA (2011) modified box-counting method to estimate the fractal dimensions. In: Applied Mechanics and Materials. Trans Tech Publ:1756–1761

Xu Y, Liu S (1999) Fractal character of grain-size distribution of expansive soils. Fractals 7:359–366

Xu Y, Matsuoka H, Sun D (2003) Swelling characteristics of fractal-textured bentonite and its mixtures. Appl Clay Sci 22:197–209

Xu Y, Da S, Yao Y (2004) Surface fractal dimension of bentonite and its application to determination of swelling properties Chaos. Solitons & Fractals 19:347–356

Xu Y, Xiang G, Jiang H, Chen T, Chu F (2014) Role of osmotic suction in volume change of clays in salt solution. Appl Clay Sci 101:354–361

Xu Y, Yu X, Xu B, Peng D, Guo X (2020) Sorption of pharmaceuticals and personal care products on soil and soil components: Influencing factors and mechanisms. Sci Total Environ:141891

Yang X, Wang M (2020) Fractal dimension analysis of aggregate packing process: A numerical case study on concrete simulation. Constr Build Mater:121376

Ye W-M, Cui Y-J, Qian L-X, Chen B (2009) An experimental study of the water transfer through confined compacted GMZ bentonite. Eng Geol 108:169–176

Ye W-M, Chen Y-G, Chen B, Wang Q, Wang J (2010a) Advances on the knowledge of the buffer/backfill properties of heavily-compacted GMZ bentonite. Eng Geol 116:12–20

Ye W, Zhang Y, Chen B, Zhou X, Xie Q (2010b) Shear strength of an unsaturated weakly expansive soil. J Rock Mech Geotech Eng 2: 155–161

Ye W-M, Lai X, Liu Y, Chen Y-G, Cui Y-J (2013) Ageing effects on swelling behaviour of compacted GMZ01 bentonite. Nucl Eng Des 265:262–268

Ye W, Borrell N, Zhu J, Chen B, Chen Y (2014) Advances on the investigation of the hydraulic behavior of compacted GMZ bentonite. Eng Geol 169:41–49

Ye Y-X, W-l Z, Han Z, Liu X-W (2019) Predicting the entire soil-water characteristic curve using measurements within low suction range. J Mt Sci 16:1198–1214

Yokozeki K (2007) Leaching from cementitious materials used in radioactive waste disposal sites. In: Thermodynamics. Elsevier, Solubility and Environmental Issues, pp 169–186

Yoon S, Jeon J-S, Kim G-Y, Seong J-H, Baik M-H (2019) Specific heat capacity model for compacted bentonite buffer materials. Ann Nucl Energy 125:18–25

Young IM, Crawford JW, Rappoldt C (2001) New methods and models for characterising structural heterogeneity of soil. Soil Tillage Res 61:33–45

Yu C (2006) Volume change behavior and its micro-structural mechanical of unsaturated GMZ bentonite Tongji University (in Chinese)

Yu H, Da S, Tian H (2019) NMR-based analysis of shear strength of weakly expansive clay in sodium chloride solution. Magn Reson Imaging 58:6–13

Zeng Y, Payton R, Gantzer C, Anderson SH (1996) Fractal dimension and lacunarity of bulk density determined with X-ray computed tomography. Soil Sci Soc Am J 60:1718–1724

Zeng Q, Li K, Fen-Chong T, Dangla P (2010) Surface fractal analysis of pore structure of high-volume fly-ash cement pastes. Appl Surf Sci 257:762–768

Zeng Q, Luo M, Pang X, Li L, Li K (2013) Surface fractal dimension: an indicator to characterize the microstructure of cement-based porous materials. Appl Surf Sci 282:302–307

Zhai Q, Rahardjo H, Satyanaga A, Dai G (2019) Estimation of unsaturated shear strength from soil–water characteristic curve. Acta Geotech 14:1977–1990

Zhang L-M (2002) Fractal characteristics of granularity distributions of aqueous bentonite and bentonite–polymer muds. Colloids Surf A Physicochem Eng Asp 202:1–7

Zhang C, Liu X, Liu Q (2013) A thermo-hydro-mechano-chemical formulation for modeling water transport around a ventilated tunnel in an argillaceous rock. J Rock Mech Geotech Eng 5:145–155

Zhang S, Tang S, Tang D, Huang W, Pan Z (2014) Determining fractal dimensions of coal pores by FHH model: problems and effects. Journal of Natural Gas Science and Engineering 21:929–939

Zhang F, Ye W-M, Chen Y-G, Chen B, Cui Y-J (2016) Influences of salt solution concentration and vertical stress during saturation on the volume change behavior of compacted GMZ01 bentonite. Eng Geol 207:48–55

Zhang F, Ye W-M, Wang Q, Chen Y-G, Chen B (2019a) An insight into the swelling pressure of GMZ01 bentonite with consideration of salt solution effects. Eng Geol 251:190–196

Zhang J, Da S, Yu H, Jiang J, Xu Y (2019b) Swelling of unsaturated GMZ07 bentonite at different temperatures. Bull Eng Geol Environ: 1–11

Zhang Z, Ye W-M, Liu Z-R, Wang Q, Cui Y-J (2020) Mechanical behavior of GMZ bentonite pellet mixtures over a wide suction range. Eng Geol 264:105383

Zhi-jian W (2005) Selection and basic properties of China's buffer materials for high level radioactive waste repository. Acta Petrol Mineral 6:583–586

Zhi-jian W (2009) Engineering materials for high level radioactive waste repository. [J] World Nuclear Geoscience:1

Zuo R, Chen M, Lin Y, Yang J, Jin S, Yue W, Wang J, Teng Y (2019) Effect of a humic acid colloid on the sorption behaviour of Sr onto soil in a candidate high-level radioactive waste geological disposal site. Environ Sci Pollut Res 26:25235–25246